

The Landscape of the Hubbard Model

Subir Sachdev

Department of Physics, Harvard University, Cambridge MA 02138

(Dated: February 5, 2022)

Abstract

I present a pedagogical survey of a variety of quantum phases of the Hubbard model. The honeycomb lattice model has a conformal field theory connecting the semi-metal to the insulator with Néel order. States with fractionalized excitations are linked to the deconfined phases of gauge theories. I also consider the confining phases of such gauge theories, and show how Berry phases of monopoles induce valence bond solid order. The triangular lattice model can display a metal-insulator transition from a Fermi liquid to a deconfined spin liquid, and I describe the theory of this transition. The bilayer triangular lattice is used to illustrate another compressible metallic phase, the ‘fractionalized Fermi liquid’. I make numerous connections of these phases and critical points to the AdS/CFT correspondence. In particular, I argue that two recent holographic constructions connect respectively to the Fermi liquid and fractionalized Fermi liquid phases.

TASI Lectures (Boulder, June 2010)

Chandrasekhar Lecture Series and Discussion Meeting on ‘‘Strongly Correlated Systems and AdS/CFT’’ (International Center for Theoretical Science (ICTS), Bangalore, Dec 2010)

I. INTRODUCTION

The Hubbard model is the simplest of a class of models describing electrons moving on a lattice with repulsive electron-electron interactions. Despite its apparent simplicity, it has become clear in the past two decades that it can display a very rich phase diagram, with a plethora of interesting phases. The most common phase is, of course, the Fermi liquid (FL), which is adiabatically connected to the metallic phase of non-interacting electrons. However, electron-electron interactions can break one or more symmetries of the Hamiltonian, and this leads to phases such as antiferromagnets, charge or spin density waves, or superconductors. Also of great interest are quantum phases which do not break any symmetries, but are nevertheless qualitatively distinct from the non-interacting electron states: such states are characterized by emergent gauge excitations, fractionalization of quasiparticle excitations, and non-trivial ground state degeneracies which depend upon the global topology of the lattice—it is often stated that such states have ‘topological’ order. Finally, there are interesting quantum phase transitions between such phases, and such quantum critical points are often described by strongly-coupled quantum field theories. In some cases, the quantum critical points can broaden into gapless quantum critical phases.

This article will present a pedagogical review of a small sample of this landscape of phases and critical points. My aim is to describe the appearance of a variety of non-trivial phases in the simplest possible context. For the honeycomb lattice with a density of one electron per site, such phases naturally have low energy excitations which have a relativistic form at low energies. Consequently, in the vicinity of quantum phase transitions, such phases and their critical points are amenable to a description by relativistic quantum field theories. In some cases, the critical points are also conformally invariant, and so are described by conformal field theories (CFTs). In these cases, the AdS/CFT correspondence can be directly applied, and I will describe the insights that have been gained from such an approach.

However, once we move away from commensurate electron densities, the quantum phases and critical points of electron lattice models rarely have any relativistic invariance in their low energy theory. I will describe here the simplest examples of ‘topologically ordered’ phases at generic electron densities. It is important to note that the lack of relativistic invariance does not rule out application of the AdS/CFT correspondence. We can begin from a relativistically invariant gravity dual theory and dope it with charge carriers by turning on a chemical potential: then even the gravity theory is not relativistically invariant at low energies, and we can hope to match its low energy physics to a condensed matter system. There has been a large effort to apply the AdS/CFT correspondence along this direction in the past few years. I have discussed some of this work in another recent review article¹, which should be viewed as a companion to the present article. I will also discuss the generic density phases here, with an emphasis on the general low energy structure of the ‘fractionalized Fermi liquid’ (FL*) phase^{2,3}, which I believe is closely related to the generic density phases that have appeared using the AdS/CFT correspondence⁴. Further details on

the connection of these phases of Hubbard-like models and the AdS/CFT correspondence appear in a recent paper⁵.

I begin by introducing the Hubbard model. It is defined by the Hamiltonian

$$H = - \sum_{i,j} t_{ij} c_{i\alpha}^\dagger c_{j\alpha} + \sum_i \left[-\mu (n_{i\uparrow} + n_{i\downarrow}) + U_i \left(n_{i\uparrow} - \frac{1}{2} \right) \left(n_{i\downarrow} - \frac{1}{2} \right) \right]. \quad (1.1)$$

Here $c_{i\alpha}$, $\alpha = \uparrow, \downarrow$ are annihilation operators on the site i of a regular lattice, and t_{ij} is a Hermitian, short-range matrix containing the ‘hopping matrix elements’ which move the electrons between different lattice sites. The density of electrons is controlled by the chemical potential μ which couples to the total electron density, with

$$n_{i\uparrow} \equiv c_{i\uparrow}^\dagger c_{i\uparrow} \quad , \quad n_{i\downarrow} \equiv c_{i\downarrow}^\dagger c_{i\downarrow}. \quad (1.2)$$

The electrons repel each other with an on-site interaction U_i ; in most cases we will take $U_i = U$ site-independent, but it will also be useful later to allow for a site-dependent U_i . For completeness, we also note the algebra of the fermion operators:

$$\begin{aligned} c_{i\alpha} c_{j\beta}^\dagger + c_{j\beta}^\dagger c_{i\alpha} &= \delta_{ij} \delta_{\alpha\beta} \\ c_{i\alpha} c_{j\beta} + c_{j\beta} c_{i\alpha} &= 0. \end{aligned} \quad (1.3)$$

The equations (1.1), (1.2), and (1.3) constitute a self-contained and complete mathematical statement of the problem of the landscape of the Hubbard model. It is remarkable that a problem that is so simple to state has such a rich phase structure as a function of the lattice choice, the fermion density, and the spatial forms of t_{ij} and U_i .

Sections II, IV, and V will deal exclusively with the honeycomb lattice at a density of one electron per site (“half-filling”), so that $\langle n_{i\uparrow} \rangle = \langle n_{i\downarrow} \rangle = 1/2$. The emphasis on the honeycomb lattice is not motivated by its particular physical importance (although, it is the lattice of graphene), but by its simplicity as a context for introducing various technical methods, quantum phases and critical points. In Section II, we will consider the semi-metal and the insulating antiferromagnet, and show that a phase transition between them is described by a relativistic field theory, which is a version of the Gross-Neveu-Yukawa model; Section III will use this field theory to present a general discussion of the physics at non-zero temperatures in the vicinity of a quantum critical point. We will focus on the transport of conserved charges, and describe insights gained from the AdS/CFT correspondence. Section IV will consider the problem of restoring the spin rotation symmetry from the antiferromagnet, while remaining in an insulating phase: this will lead to a description in terms of a U(1) gauge theory, and the appearance of an insulating phase with valence bond solid (VBS) order. Finally, Section V will combine all the phases of the half-filled honeycomb lattice discussed so far in a single phase diagram: this will require introduction of a SU(2) gauge

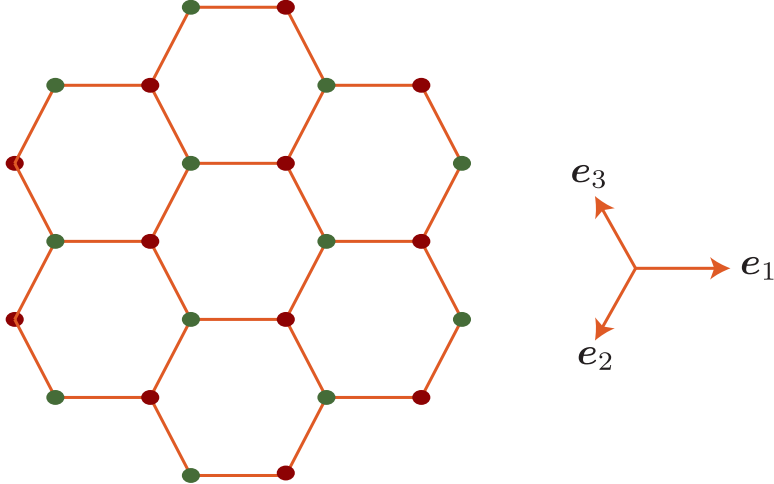


FIG. 1: The honeycomb lattice with its A (green) and B (red) sublattices

theory. We will find an interesting multi-critical point in Section V, which has many features in common with the supersymmetric CFTs studied using the AdS/CFT correspondence.

Sections IV and V can be skipped in a first reading, without significant loss of continuity.

We will move away from half-filling in Sections VI and VII, where we will turn our attention to metallic phases with Fermi surfaces. Section VI considers the Hubbard model on the triangular lattice, and describes a phase diagram which includes Fermi liquid (FL) and spin liquid phases. Section VII extends our discussion to the the Hubbard model on a bilayer triangular lattice, which has been realized in experiments⁶ on ³He. Here we will present a gauge theory of another metallic phase, the fractionalized Fermi liquid (FL*). We will also discuss the connections to compressible metallic phases obtained using the AdS/CFT correspondence, complementing the recent discussion in Ref. 5.

II. SEMI-METAL AND ANTIFERROMAGNETISM ON THE HONEYCOMB LATTICE

A. Preliminaries

We will consider the Hubbard model (1.1) with the sites i on locations \mathbf{r}_i on the honeycomb lattice shown in Fig. 1. Here, we set up some notation allowing us to analyze the geometry of this lattice.

We work with a lattice with unit nearest neighbor spacing. We define unit length vectors which connect nearest-neighbor sites

$$\mathbf{e}_1 = (1, 0) \quad , \quad \mathbf{e}_2 = (-1/2, \sqrt{3}/2) \quad , \quad \mathbf{e}_3 = (-1/2, -\sqrt{3}/2). \quad (2.1)$$

Note that $\mathbf{e}_i \cdot \mathbf{e}_j = -1/2$ for $i \neq j$, and $\mathbf{e}_1 + \mathbf{e}_2 + \mathbf{e}_3 = 0$. The lattice can be divided into the

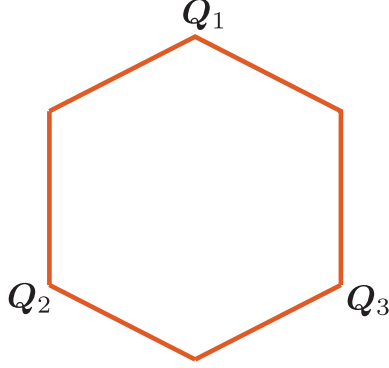


FIG. 2: The first Brillouin zone of the honeycomb lattice.

A and B sublattices, as shown in Fig. 1. We take the origin of co-ordinates of the lattice at the center of an *empty hexagon*. The A sublattice sites closest to the origin are at \mathbf{e}_1 , \mathbf{e}_2 , and \mathbf{e}_3 , while the B sublattice sites closest to the origin are at $-\mathbf{e}_1$, $-\mathbf{e}_2$, and $-\mathbf{e}_3$.

The unit cell of the hexagonal lattice contains 2 sites, one each from the A and B sublattices. These unit cells form a triangular Bravais lattice consisting of the centers of the hexagons. The triangular lattice points closest to the origin are $\pm(\mathbf{e}_1 - \mathbf{e}_2)$, $\pm(\mathbf{e}_2 - \mathbf{e}_3)$, and $\pm(\mathbf{e}_3 - \mathbf{e}_1)$. The reciprocal lattice is a set of wavevectors \mathbf{G} such that $\mathbf{G} \cdot \mathbf{r} = 2\pi \times \text{integer}$, where \mathbf{r} is the center of any hexagon of the honeycomb lattice. The reciprocal lattice is also a triangular lattice, and it consists of the points $\sum_i n_i \mathbf{G}_i$, where n_i are integers and

$$\mathbf{G}_1 = \frac{4\pi}{3}\mathbf{e}_1 \quad , \quad \mathbf{G}_2 = \frac{4\pi}{3}\mathbf{e}_2 \quad , \quad \mathbf{G}_3 = \frac{4\pi}{3}\mathbf{e}_3. \quad (2.2)$$

The unit cell of the reciprocal lattice is called the first Brillouin zone. This is a hexagon whose vertices are given by

$$\mathbf{Q}_1 = \frac{1}{3}(\mathbf{G}_2 - \mathbf{G}_3) \quad , \quad \mathbf{Q}_2 = \frac{1}{3}(\mathbf{G}_3 - \mathbf{G}_1) \quad , \quad \mathbf{Q}_3 = \frac{1}{3}(\mathbf{G}_1 - \mathbf{G}_2), \quad (2.3)$$

and $-\mathbf{Q}_1$, $-\mathbf{Q}_2$, and $-\mathbf{Q}_3$; see Fig. 2. Integrals and sums over momentum space will implicitly extend only over the first Brillouin zone. This is the ‘ultraviolet cutoff’ imposed by the underlying lattice structure.

We define the Fourier transform of the electrons on the A sublattice by

$$c_{A\alpha}(\mathbf{k}) = \frac{1}{\sqrt{\mathcal{N}}} \sum_{i \in A} c_{i\alpha} e^{-i\mathbf{k} \cdot \mathbf{r}_i}, \quad (2.4)$$

where \mathcal{N} is the number of sites on one sublattice; similarly for $c_{B\alpha}$. Note that $c_{A\alpha}(\mathbf{k} + \mathbf{G}) = c_{A\alpha}(\mathbf{k})$: consequently, sums over momentum have to be restricted to the first Brillouin zone to avoid double counting. Thus the inverse of Eq. (2.4) sums over \mathbf{k} in the first Brillouin zone.

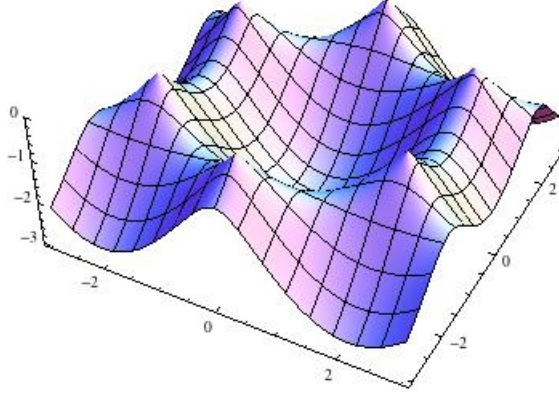


FIG. 3: The lower band of the dispersion in Eq. (2.7) for $\mu = 0$

B. Semi-metal

We begin with free electrons in the honeycomb lattice, $U = 0$, with only nearest-neighbor electron hopping $t_{ij} = t$. Using Eq. (2.4), we can write the hopping Hamiltonian as

$$\begin{aligned}
 H_0 = & -t \sum_{\mathbf{k}} \left(e^{i\mathbf{k}\cdot\mathbf{e}_1} + e^{i\mathbf{k}\cdot\mathbf{e}_2} + e^{i\mathbf{k}\cdot\mathbf{e}_3} \right) c_{A\alpha}^\dagger(\mathbf{k}) c_{B\alpha}(\mathbf{k}) + \text{H.c.} \\
 & -\mu \sum_{\mathbf{k}} \left(c_{A\alpha}^\dagger(\mathbf{k}) c_{A\alpha}(\mathbf{k}) + c_{B\alpha}^\dagger(\mathbf{k}) c_{B\alpha}(\mathbf{k}) \right)
 \end{aligned} \tag{2.5}$$

We introduce Pauli matrices τ^a ($a = x, y, z$) which act on the A, B sublattice space; then this Hamiltonian can be written as

$$\begin{aligned}
 H_0 = & \sum_{\mathbf{k}} c^\dagger(\mathbf{k}) \left[-\mu - t \left(\cos(\mathbf{k} \cdot \mathbf{e}_1) + \cos(\mathbf{k} \cdot \mathbf{e}_2) + \cos(\mathbf{k} \cdot \mathbf{e}_3) \right) \tau^x \right. \\
 & \left. + t \left(\sin(\mathbf{k} \cdot \mathbf{e}_1) + \sin(\mathbf{k} \cdot \mathbf{e}_2) + \sin(\mathbf{k} \cdot \mathbf{e}_3) \right) \tau^y \right] c(\mathbf{k}),
 \end{aligned} \tag{2.6}$$

where the sublattice and spin indices on the electrons are now implicit: the $c(\mathbf{k})$ are 4-component fermion operators.

The energy eigenvalues are easily determined to be

$$-\mu \pm \left| e^{i\mathbf{k}\cdot\mathbf{e}_1} + e^{i\mathbf{k}\cdot\mathbf{e}_2} + e^{i\mathbf{k}\cdot\mathbf{e}_3} \right| \tag{2.7}$$

and these are plotted in Fig. 3. At half-filling, exactly half the states should be occupied in the ground state, and for the spectrum in Eq. (2.7) this is achieved at $\mu = 0$.

A crucial feature of any metallic state is the Fermi surface: this is boundary between the occupied and empty states in momentum space. In two spatial dimensions, this boundary is generically a line in momentum space, and this is the case for the dispersion in Eq. (2.7)

for $\mu \neq 0$. However, for the $\mu = 0$, the honeycomb lattice has the special property that the occupied and empty states meet only at a discrete set of single points in momentum space: this should be clear from the dispersion plotted in Fig. 3. Only 2 of these points are distinct, in that they are not separated by a reciprocal lattice vector \mathbf{G} . So the half-filled honeycomb lattice has 2 ‘Fermi points’, and realizes a ‘semi-metal’ phase. The low energy excitations of the semi-metal consist of particles and holes across the Fermi point, and these have a lower density of states than in a metallic phase with a Fermi line. We also note that the Fermi-point structure is protected by a sublattice exchange symmetry: it is not special to the nearest-neighbor hopping model, and it also survives the inclusion of electron-electron interactions.

We obtain a very useful, and universal, theory for the low energy excitations of the semi-metal by expanding (2.6) in the vicinity of the Fermi points. The distinct Fermi points are present at \mathbf{Q}_1 and $-\mathbf{Q}_1$; all other Fermi points are separated from these two points by a reciprocal lattice vector \mathbf{G} . So we define continuum Fermi field which reside in ‘valleys’ in the vicinity of these points by

$$\begin{aligned} C_{A1\alpha}(\mathbf{k}) &= \sqrt{A} c_{A\alpha}(\mathbf{Q}_1 + \mathbf{k}) \\ C_{A2\alpha}(\mathbf{k}) &= \sqrt{A} c_{A\alpha}(-\mathbf{Q}_1 + \mathbf{k}) \\ C_{B1\alpha}(\mathbf{k}) &= \sqrt{A} c_{B\alpha}(\mathbf{Q}_1 + \mathbf{k}) \\ C_{B2\alpha}(\mathbf{k}) &= \sqrt{A} c_{B\alpha}(-\mathbf{Q}_1 + \mathbf{k}), \end{aligned} \quad (2.8)$$

where A is the total area of the honeycomb lattice, and the momentum \mathbf{k} is small. The field C is a 8-component continuum canonical Fermi field: the components correspond to spin (\uparrow, \downarrow), sublattice (A, B), and valley (1, 2) indices. We will also use Pauli matrices which act on the spin (σ^a), sublattice (τ^a), and valley (ρ^a) space.

Inserting Eq. (2.8) into Eq. (2.6), we obtain the continuum Hamiltonian

$$H_0 = \int \frac{d^2k}{4\pi^2} C^\dagger(\mathbf{k}) \left(v\tau^y k_x + v\tau^x \rho^z k_y \right) C(\mathbf{k}), \quad (2.9)$$

where $v = 3t/2$. From now on we rescale time to set $v = 1$. Diagonalizing Eq. (2.9), we obtain the relativistic spectrum

$$\pm \sqrt{k_x^2 + k_y^2}, \quad (2.10)$$

which corresponds to the values of Eq. (2.7) near the Fermi points.

The relativistic structure of H_0 can be made explicit by rewriting it as the Lagrangian of massless Dirac fermions. Define $\bar{C} = C^\dagger \rho^z \tau^z$. Then we can write the Euclidean time (τ) Lagrangian density of the semi-metal phase as

$$\mathcal{L}_0 = \bar{C} (\partial_\tau \gamma_0 + \partial_x \gamma_1 + \partial_y \gamma_2) C \quad (2.11)$$

where ω is the frequency associated with imaginary time, and the Dirac γ matrices are

$$\gamma_0 = -\rho^z \tau^z \quad \gamma_1 = \rho^z \tau^x \quad \gamma_2 = -\tau^y. \quad (2.12)$$

In addition to relativistic invariance, this form makes it clear the free-fermion Lagrangian has a large group of ‘flavor’ symmetries that acts on the 8×8 fermion space and commute with the γ matrices. Most of these symmetries are not obeyed by higher-order gradients, or by fermion interaction terms which descend from the Hubbard model.

Let us now turn on a small repulsion, U , between the fermions in the semi-metal. Because of the point-like nature of the Fermi surface, it is easier to determine the consequences of this interaction here than in a metallic phase with a Fermi line of gapless excitations. We can use traditional renormalization group (RG) methods to conclude that a weak U is irrelevant in the infrared: the computation is left as an exercise below. Consequently, the semi-metal state is a stable phase which is present over a finite range of parameters.

Exercise: Observe that \mathcal{L}_0 is invariant under the scaling transformation $x' = xe^{-\ell}$ and $\tau' = \tau e^{-\ell}$. Write the Hubbard interaction U in terms of the Dirac fermions, and show that it has the tree-level scaling transformation $U' = Ue^{-\ell}$. So argue that all short-range interactions are *irrelevant* in the Dirac semi-metal phase.

C. Antiferromagnet

Although a small U is irrelevant, new phases can and do appear at large U . To see this, let us return to the lattice Hubbard model in Eq. (1.1), and consider the limit of large $U_i = U$. We will assume $\mu = 0$ and half-filling in the remainder of this section.

At $U = \infty$, the eigenstates are simple products over the states on each site. Each site has 4 states:

$$|0\rangle \quad , \quad c_{i\uparrow}^\dagger |0\rangle \quad , \quad c_{i\downarrow}^\dagger |0\rangle \quad , \quad c_{i\uparrow}^\dagger c_{i\downarrow}^\dagger |0\rangle, \quad (2.13)$$

where $|0\rangle$ is the empty state. The energies of these states are $U/4$, $-U/4$, $-U/4$, and $U/4$ respectively. Thus the ground state on each site is doubly-degenerate, corresponding to the spin-up and spin-down states of a single electron. The lattice model has a degeneracy of $2^{2\mathcal{N}}$, and so a non-zero entropy density (recall that \mathcal{N} is the number of sites on one sublattice).

Any small perturbation away from the $U = \infty$ limit is likely to lift this exponential large degeneracy. So we need to account for the electron hopping t . At first order, electron hopping moves an electron from one singly-occupied site to another, yielding a final state with one empty and one doubly occupied site. This final state has an energy U higher than the initial state, and so is not part of the low energy manifold. So by the rules of degenerate perturbation theory, there is no correction to the energy of all the $2^{2\mathcal{N}}$ ground states at first

order in t .

At second order in t , we have to use the effective Hamiltonian method. This performs a canonical transformation to eliminate the couplings from the ground states to all the states excited by energy U , while obtaining a modified Hamiltonian which acts on the 2^{2N} ground states. This method is described in text books on quantum mechanics, and we leave its application here as an exercise. The resulting effective Hamiltonian is the Heisenberg antiferromagnet:

$$H_J = \sum_{i<j} J_{ij} S_i^a S_j^a \quad , \quad J_{ij} = \frac{4t_{ij}^2}{U}, \quad (2.14)$$

where J_{ij} is the exchange interaction and S_i^a are the spin operators on site i

$$S_i^a = \frac{1}{2} c_{i\alpha}^\dagger \sigma_{\alpha\beta}^a c_{i\beta}. \quad (2.15)$$

Note that these spin operators preserve the electron occupation number on every site, and so act within the subspace of the 2^{2N} low energy states. The Hamiltonian H_J lifts the macroscopic degeneracy, and the entropy density of the new ground state will be zero.

Exercise: Use the effective Hamiltonian method described in Ref. 7 to obtain Eq. (2.14). At second order in U , it is sufficient to consider the 2-site Hubbard model. This has a total of 16 states, and 4 ground states at $U = \infty$. Derive the effective Hamiltonian which acts on these 4 states at order t^2 .

Although we cannot compute the exact ground state of H_J on the honeycomb lattice with nearest-neighbor exchange, numerical studies⁸ leave little doubt to its basic structure. The ground state is adiabatically connected to that obtained by treating the S_i^a as classical vectors in spin space: it has antiferromagnetic (or Néel) order which breaks the global SU(2) spin rotation symmetry, by a spontaneous polarization of the spins on opposite orientations on the two sublattices

$$\eta_i \langle S_i^a \rangle = N^a, \quad (2.16)$$

where $\eta_i = 1$ ($\eta_i = -1$) on sublattice A (B), and N^a is the vector Néel order parameter; see Fig. 4. Classically this state minimizes the exchange coupling in Eq. (2.14) because $J_{ij} > 0$. Quantum fluctuations for spin $S = 1/2$ reduce the spontaneous moment from its classical value, but a non-zero moment remains on the honeycomb lattice.

What is the electronic excitation spectrum in the antiferromagnet? To determine this, it is useful to write the Néel order parameter in terms of the continuum Dirac fields introduced in Section II B. We observe

$$\sum_i \eta_i S_i^a = \sum_{\mathbf{k}} \left(c_{A\alpha}^\dagger \sigma_{\alpha\beta}^a c_{A\beta} - c_{B\alpha}^\dagger \sigma_{\alpha\beta}^a c_{B\beta} \right) = \int \frac{d^2k}{4\pi^2} C^\dagger \tau^z \sigma^a C \quad (2.17)$$

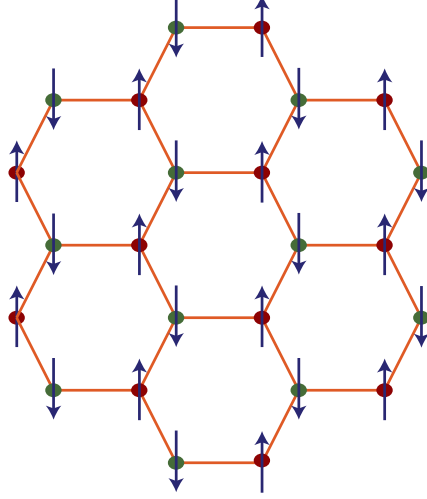


FIG. 4: The large U state with antiferromagnetic (Néel) order.

Thus the Néel order parameter N^a is given by the fermion bilinear

$$N^a = \langle C^\dagger \tau^z \sigma^a C \rangle = \langle \bar{C} \rho^z \sigma^a C \rangle, \quad (2.18)$$

and the vacuum expectation value (VEV) is non-zero in the antiferromagnet. We can expect that electron-electron interactions will induce a coupling between the fermion excitations and this VEV in the low energy Hamiltonian for the Néel phase. Choosing Néel ordering in the z direction

$$N^a = N_0 \delta_{az}, \quad (2.19)$$

we anticipate that H_0 in Eq. (2.9) is modified in the Néel phase to

$$H_N = \int \frac{d^2 k}{4\pi^2} C^\dagger(\mathbf{k}) \left(\tau^y k_x + \tau^x \rho^z k_y - \lambda N_0 \tau^z \sigma^z \right) C(\mathbf{k}), \quad (2.20)$$

where λ is a coupling determined by the electron interactions, and we have assumed Néel order polarized in the z direction. This effective Hamiltonian will be explicitly derived in the next subsection. We can now easily diagonalize H_N to deduce that the electronic excitations have energy

$$\pm \sqrt{k_x^2 + k_y^2 + \lambda^2 N_0^2}. \quad (2.21)$$

This is the spectrum of massive Dirac fermions. So the Fermi point has disappeared, and an energy gap has opened in the fermion excitation spectrum. In condensed matter language, the phase with antiferromagnetic order is an insulator, and not a semi-metal: transmission of electronic charge will require creation of gapped particle and hole excitations.

D. Quantum phase transition

We have now described a semi-metal phase for small U , and an antiferromagnetic insulator for large U . Both are robust phases, whose existence has been reliably established. We now consider connecting these two phases at intermediate values of U . This is a complex subject, and careful numerical studies are only just emerging for the model with nearest-neighbor hopping⁸. It is already clear, however, that by varying the form of the microscopic coupling we can obtain a rich variety of intermediate phases^{9–14}. In the present subsection we consider the simplest possibility: there are no new intermediate phases, and only a direct quantum phase transition between the semi-metal and the antiferromagnetic insulator^{15–17}.

We can derive the field theory for this direct transition either by symmetry considerations, or by an explicit derivation from the Hubbard model. Let us initially follow the second route. We start with the Hubbard Hamiltonian in Eq. (1.1), use the operator identity (valid on each site i):

$$U \left(n_{\uparrow} - \frac{1}{2} \right) \left(n_{\downarrow} - \frac{1}{2} \right) = -\frac{2U}{3} S_i^{a2} + \frac{U}{4}. \quad (2.22)$$

Then, in the fermion coherent state path integral for the Hubbard model, we apply a ‘Hubbard-Stratonovich’ transformation to the interaction term; this amounts to using the identity

$$\begin{aligned} & \exp \left(\frac{2U}{3} \sum_i \int d\tau S_i^{a2} \right) \\ &= \int \mathcal{D}X_i^a(\tau) \exp \left(- \sum_i \int d\tau \left[\frac{3}{8} X_i^{a2} - \sqrt{U} X_i^a S_i^a \right] \right) \end{aligned} \quad (2.23)$$

The fermion path integral is now a bilinear in the fermions, and we can, at least formally, integrate out the fermions in the form of a functional determinant. We imagine doing this temporarily, and then look for the saddle point of the resulting effective action for the X_i^a . At the saddle-point we find that the lowest energy is achieved when the vector has opposite orientations on the A and B sublattices. Anticipating this, we look for a continuum limit in terms of a field φ^a where

$$X_i^a = \eta_i \varphi^a \quad (2.24)$$

Using Eq. (2.17), the continuum limit of the coupling between the field φ^a and the fermions in Eq. (2.23) is given by

$$X_i^a c_{i\alpha}^\dagger \sigma_{\alpha\beta}^a c_{i\beta} = \varphi^a C^\dagger \tau^z \sigma^a C = \varphi^a \bar{C} \rho^z \sigma^a C \quad (2.25)$$

From this it is clear that φ^a is a dynamical quantum field which represents the fluctuations of the local Néel order, and

$$\langle \varphi^a \rangle \propto N^a. \quad (2.26)$$

Now we can take the continuum limit of all the terms in the coherent state path integral for the lattice Hubbard model and obtain the following continuum Lagrangian density

$$\mathcal{L} = \bar{C}\gamma_\mu\partial_\mu C + \frac{1}{2} [(\partial_\mu\varphi^a)^2 + s\varphi^{a2}] + \frac{u}{24} (\varphi^{a2})^2 - \lambda\varphi^a\bar{C}\rho^z\sigma^a C \quad (2.27)$$

This is a relativistic quantum field theory for the 8-component fermion field C and the 3-component real scalar φ^a , related to the Gross-Neveu-Yukawa model. We have included gradient terms and quartic in the Lagrangian for φ^a : these are not present in the derivation outlined above from the lattice Hubbard model, but are clearly induced by higher energy fermions are integrated out. The Lagrangian includes various phenomenological couplings constants (s, u, λ); as these constants are varied, \mathcal{L} can describe *both* the semi-metal and insulating antiferromagnet phases, and also the quantum critical point between them.

Note that the matrix $\rho^z\sigma^a$ commutes with all the γ_μ ; hence $\rho^z\sigma^a$ is a matrix in “flavor” space. So if we consider C as 2-component Dirac fermions, then these Dirac fermions carry an additional 4-component flavor index.

The semi-metal phase is the one where φ^a has vanishing VEV. In mean-field theory, this appears for $s > 0$. The φ^a excitations are then massive, and these constitute a triplet of gapped ‘spin-excitons’ associated with fluctuations of the local antiferromagnetic order. The Dirac fermions are massless, and represent the Fermi point excitations of the semi-metal.

The Néel phase has a non-zero VEV, $\langle\varphi^a\rangle \neq 0$, and appears in mean-field theory for $s < 0$. Here the Dirac fermions acquire a gap, indicating that the Fermi point has vanished, and we are now in an insulating phase. The fluctuations of φ are a doublet of Goldstone modes (‘spin waves’) and a longitudinal massive Higgs boson.

Finally, we are ready to address the quantum critical point between these phases. In mean-field theory, this transition occurs at $s = 0$. As is customary in condensed matter physics, it is useful to carry out an RG analysis near this point. The tree-level analysis is carried out in the following exercise.

Exercise: Perform a tree-level RG transformation on \mathcal{L} . The quadratic gradient terms are invariant under $C' = Ce^\ell$ and $\varphi' = \varphi e^{\ell/2}$. Show that this leads to $s' = se^{2\ell}$. Thus s is a relevant perturbation which drives the system into either the semi-metal or antiferromagnetic insulator. The quantum critical point is reached by tuning s to its critical value (= 0 at tree level). Show that the couplings u and λ are both relevant perturbations at this critical point. Thus, while interactions are irrelevant in the Dirac semi-metal (and in the insulator), they are strongly relevant at the quantum-critical point.

Further study of this quantum critical point requires a RG analysis which goes beyond tree-level. Such an analysis can be controlled in an expansion in $1/N$ (where N is the number of fermion flavors) or $(3 - d)$ (where d is the spatial dimensionality). For reviews see Ref. 18 or Chapter 17 of Ref. 19. The main conclusion of such analyses is that there is

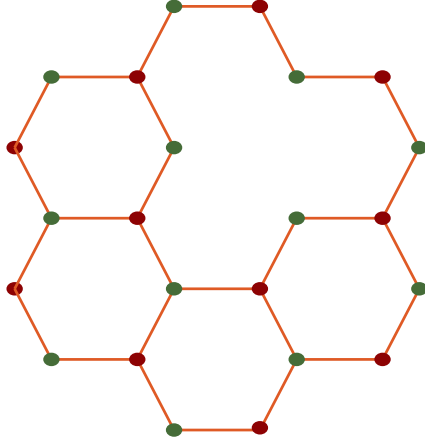


FIG. 5: The honeycomb lattice with a vacancy.

an RG fixed point at which the φ^{a2} is the only relevant perturbation. Non-linearities such as λ and u all reach stable fixed point values of order unity. This non-trivial fixed point implies that the physics of the quantum critical point is highly non-trivial and strongly coupled. The RG fixed point is scale- and relativistic-invariant, and this implies that it is also conformally invariant. Thus the quantum critical point is described by a CFT in 2+1 spacetime dimensions: a CFT3.

We will not describe the critical theory in any detail here. However, we will note some important characteristics of correlation functions at the quantum critical point. The electron Green's function has the following structure

$$\langle C(k, \omega); C^\dagger(k, \omega) \rangle \sim \frac{i\omega + k_x \tau^y + k_y \tau^x \rho^z}{(\omega^2 + k_x^2 + k_y^2)^{1-\eta/2}} \quad (2.28)$$

where $\eta > 0$ is the *anomalous dimension* of the fermion. This leads to a fermion spectral density which has no quasiparticle pole: thus the quantum critical point has no well-defined quasiparticle excitations. This distinguishes it from both the semi-metal and insulating antiferromagnetic phases that flank it on either side: both had excitations with infinitely-sharp quasiparticle peaks. Similar anomalous dimensions appear in the correlations of the bosonic order parameter φ^a .

E. Quantum impurities

We briefly note the physics of quantum impurities in the honeycomb lattice, which were discussed more completely in the companion review¹. The translational invariance of the honeycomb lattice will be broken *only* in this subsection.

Imagine removing a single atom from the honeycomb lattice, as shown in Fig. 5. At $U = 0$, the electronic spectrum of such a lattice was described in Ref. 20. They showed that there

was a quasi-localized state in the vicinity of the impurity exactly at zero energy, which decayed as $1/r$ at a distance r from the impurity. Upon including U , we expect this state to capture a single electron whose $S = 1/2$ spin interacts with the bulk excitations.

Let us represent the impurity by a localized fermion operator $\chi_\alpha(\tau)$. Note that this fermion has no dependence upon the spatial co-ordinate \mathbf{r} , and is a function only of the time τ . Now we can couple this fermion to the bulk excitations which were described by \mathcal{L} in Eq. (2.27) in the vicinity of the semi-metal to antiferromagnetic insulator transition. The full system is described by the Lagrangian $\mathcal{L} + \mathcal{L}_{\text{imp}}$ where

$$\mathcal{L}_{\text{imp}} = \chi_\alpha^\dagger \frac{\partial \chi_\alpha}{\partial \tau} - h \chi_\alpha^\dagger \sigma_{\alpha\beta}^a \chi_\beta \varphi^a(\mathbf{r} = 0, \tau); \quad (2.29)$$

note that whereas the Lagrangian \mathcal{L} is integrated over spacetime, the Lagrangian \mathcal{L}_{imp} is only integrated over time. There are many possible couplings between the impurity and bulk degrees of freedom which are allowed by the symmetry of the problem, but we have only included a single one. This is easily seen to be the only term which is relevant under the RG which applies in the vicinity of the bulk quantum phase transition.

The RG flow of the bulk-impurity coupling h was described in Refs. 21–23. It was found that h approached a fixed-point coupling in the infrared, just like the couplings u and λ in \mathcal{L} . Thus no new couplings are necessary to describe the low energy physics of the impurity provided we are not too far from the semi-metal to antiferromagnetic insulator quantum critical point.

Further details of the impurity dynamics may be found in the companion review¹, where it was described for a closely related bulk quantum critical point. A close analogy was also drawn between these impurity problems and defects in super Yang-Mills theories; the latter can be solved²⁴ by intersecting brane models in string theory, and led to a description of the impurity criticality using a AdS_2 geometry.

F. Electrical transport

We now revert to the honeycomb lattice without impurities.

An important set of observables which do *not* acquire anomalous dimensions at the quantum critical point are the currents associated with global conservation laws. As the simplest example here, let us consider correlations of the conserved electric charge of the electrons, and the associated electrical conductivity σ . At zero temperature ($T = 0$), we have $\sigma = 0$ in the insulator, while the semi-metal and the quantum critical point have finite non-zero values of σ , as we will now see.

The conserved electrical current is

$$J_\mu = -i\bar{C}\gamma_\mu C. \quad (2.30)$$

Let us compute its two-point correlator, $K_{\mu\nu}(k)$ at a spacetime momentum k_μ . At leading order, this is given by a one fermion loop diagram which evaluates to

$$\begin{aligned} K_{\mu\nu}(k) &= \int \frac{d^3p}{8\pi^3} \frac{\text{Tr} [\gamma_\mu (i\gamma_\lambda p_\lambda + m\rho^z \sigma^z) \gamma_\nu (i\gamma_\delta (k_\delta + p_\delta) + m\rho^z \sigma^z)]}{(p^2 + m^2)((p+k)^2 + m^2)} \\ &= -\frac{2}{\pi} \left(\delta_{\mu\nu} - \frac{k_\mu k_\nu}{k^2} \right) \int_0^1 dx \frac{k^2 x(1-x)}{\sqrt{m^2 + k^2 x(1-x)}}, \end{aligned} \quad (2.31)$$

where the mass $m = 0$ in the semi-metal and at the quantum critical point, while $m = |\lambda N_0|$ in the insulator. Note that the current correlation is purely transverse, and this follows from the requirement of current conservation

$$k_\mu K_{\mu\nu} = 0. \quad (2.32)$$

Of particular interest to us is the K_{00} component, after analytic continuation to Minkowski space where the spacetime momentum k_μ is replaced by (ω, k) . The conductivity is obtained from this correlator via the Kubo formula

$$\sigma(\omega) = \lim_{k \rightarrow 0} \frac{-i\omega}{k^2} K_{00}(\omega, k). \quad (2.33)$$

In the insulator, where $m > 0$, analysis of the integrand in Eq. (2.31) shows that the spectral weight of the density correlator has a gap of $2m$ at $k = 0$, and the conductivity in Eq. (2.33) vanishes. These properties are as expected in any insulator.

In the metal, and at the critical point, where $m = 0$, the fermionic spectrum is gapless, and so is that of the charge correlator. The density correlator in Eq. (2.31) and the conductivity in Eq. (2.33) evaluate to the simple universal results

$$\begin{aligned} K_{00}(\omega, k) &= \frac{1}{4} \frac{k^2}{\sqrt{k^2 - \omega^2}} \\ \sigma(\omega) &= \frac{1}{4}. \end{aligned} \quad (2.34)$$

How about beyond the one-loop results? The insulator maintains a gap to charged excitations, and so the conductivity remains at zero. In the semi-metal, the fermions are gapless, but they couple only to the gapped fluctuations of the Néel order φ^a . Examination of the perturbation theory shows that these have no effect on the current correlators at small momenta and frequency, and so the results in Eq. (2.34) are *exact* in the limit of small ω and k in the semi-metal.

At the quantum critical point, we have to consider the strong critical fluctuations associated with fixed-point values of the Yukawa coupling λ and the quartic bosonic interaction u . These can be examined in the $(3-d)$ or the $1/N$ expansion, and require evaluation of multi-loop diagrams. We will not describe the computations here, but note a remarkable

feature: all divergences associated with the critical fluctuations cancel, and the final result is universal. The values of none of the couplings of the Lagrangian in Eq. (2.27) matters because these are all pinned by the RG fixed point. There are no anomalous dimensions, and the results in Eq. (2.34) generalize to

$$\begin{aligned} K_{00}(\omega, k) &= \mathcal{K} \frac{k^2}{\sqrt{k^2 - \omega^2}} \\ \sigma(\omega) &= \mathcal{K}, \end{aligned} \tag{2.35}$$

where \mathcal{K} is a universal number dependent only upon the universality class of the quantum critical point. The value of the \mathcal{K} for the Gross-Neveu-Yukawa model in Eq. (2.27) is not known exactly, but can be estimated by computations in the $(3 - d)$ or $1/N$ expansions.

III. NON-ZERO TEMPERATURES AND THE ADS/CFT CORRESPONDENCE

We begin by some general remarks on the influence of a non-zero temperature, T , on a generic, strongly-coupled quantum critical point. Let us consider a quantum-critical point which has only a single relevant perturbation, s , as is the case for the model in Eq. (2.27) (the generalization to several relevant perturbations is immediate). So near the quantum critical point, the RG flow is described by

$$\frac{ds}{d\ell} = \frac{1}{\nu} s. \tag{3.1}$$

In standard condensed matter notation, the eigenvalue of the relevant flow is written in terms of ν , the correlation length exponent. Now in the quantum field theory in Euclidean time, a non-zero T corresponds to placing the theory on a cylinder of circumference $1/T$. Such a finite size is clearly relevant in the infrared, and also indicates that $1/T$ transforms just like the temporal length under the RG. We write this as

$$\frac{dT}{d\ell} = zT, \tag{3.2}$$

where z is the dynamic critical exponent. All the theories for the honeycomb lattice at half filling have $z = 1$, but we allow z to be arbitrary here.

Eqs. (3.1) and (3.2) are of course trivial to integrate

$$s(\ell) = s e^{\ell/\nu} \quad , \quad T(\ell) = T e^{z\ell}, \tag{3.3}$$

but the results teach us an important lesson which is summarized in the canonical quantum-critical phase diagram shown in Fig. 6. We ask the question: which of the relevant perturbations, s or T , is more important? To answer this question, we integrate the RG equations

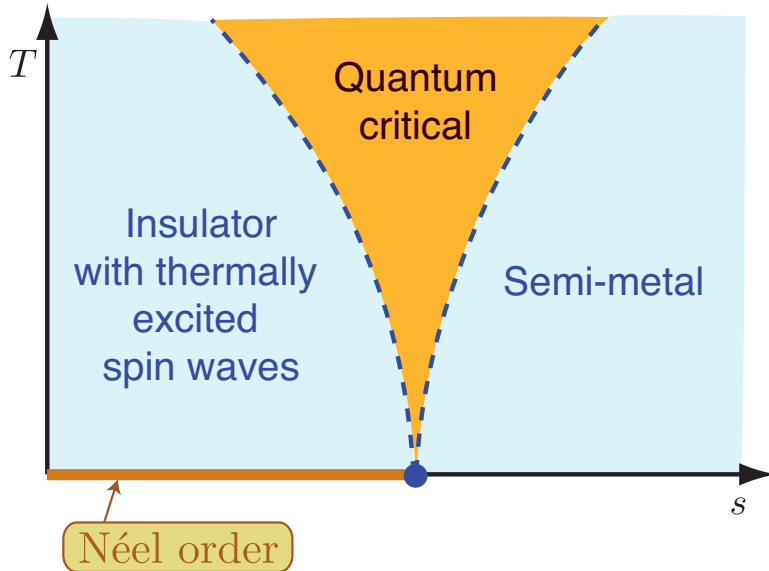


FIG. 6: Canonical quantum critical crossover phase diagram. The dashed lines occur for $T \sim |s|^{z\nu}$, and indicate crossovers between the orange- and blue-shaded regions which are generic from any strongly-coupled quantum critical point. Specific features of the blue-shaded regions for the theory Eq. (2.27) of the transition from the semi-metal to the Néel-ordered insulator are also indicated. The Néel order vanishes for any $T > 0$ because non-Abelian continuous symmetries cannot be broken in two spatial dimensions.

to a scale $\ell = \ell^*$ until the winner reaches a value of unity. This allows us to conclude that for $T > |s|^{z\nu}$, thermal effects are more important than any deviation of the coupling from the RG fixed point. Conversely, for $T < |s|^{z\nu}$ the couplings flow far from the critical fixed point before any thermally excited states need be considered. These considerations lead to the two distinct regimes show in Fig. 6.

In the blue-colored regimes of Fig. 6, where $T < |s|^{z\nu}$, the physics of the two non-critical phases dominates. For the model of Eq. (2.27), these are the semi-metal or antiferromagnetic insulator phases, both of which have well-defined quasiparticle excitations. Consequently, the long-time dynamics can be written using quasi-classical models of the interactions of these quasiparticles.

Our interest here is primarily in the orange-colored regime of quantum criticality, $T > |s|^{z\nu}$. Here T is the primary perturbation to the quantum critical theory. The deviation of the couplings from $T = 0$ RG fixed point is unimportant, and the system behaves as it is described by the universal quantum-critical Lagrangian in the entire regime. For the relativistic model considered here, the strongly coupled CFT describes the dynamics of the orange-colored region.

It has been argued¹⁹ that a central general property of quantum critical dynamics is the short time over which the system relaxes back to thermal equilibrium. We imagine perturbing the system away from equilibrium, and measuring the time, τ_{eq} over which it relaxes back to local equilibrium (the adjective ‘local’ implies that we exclude diffusion of

globally conserved charges which can take a long time to reach equilibrium across the entire system). In the regime of strongly-coupled quantum criticality this is given by

$$\tau_{\text{eq}} = \mathcal{C} \frac{\hbar}{k_B T} \quad (3.4)$$

where \mathcal{C} is a universal number dependent only upon the universality class of the transition, and precise definition used for τ_{eq} . Furthermore, in all other regimes, the value of τ_{eq} is parametrically larger than the value in Eq. (3.4). Thus quantum criticality is described by a quantum fluid with the *shortest possible* thermal equilibration time. This characteristic makes it a “nearly perfect” fluid.

It is important to note that our discussion above does *not* apply to CFTs in 1+1 dimensions. These are integrable systems, whose long-time dynamics is non-generic and does not generalize to higher dimensions.

A. Quantum critical transport

Let us explore the ideas above by examining the behavior of the electron conductivity of the model in Eq. (2.27) in the quantum-critical regime. At one-loop order, we can set $m = 0$, and then repeat the computation in Eq. (2.31) at $T > 0$. This only requires replacing the integral over the loop frequency by a summation over the Matsubara frequencies, which are quantized by odd multiples of πT . Such a computation, via Eq. (2.33) leads to the conductivity²⁵

$$\begin{aligned} \text{Re}[\sigma(\omega)] &= (2T \ln 2) \delta(\omega) + \frac{1}{4} \tanh\left(\frac{|\omega|}{4T}\right) \\ \text{Im}[\sigma(\omega)] &= \int_{-\infty}^{\infty} \frac{d\Omega}{\pi} \mathcal{P} \left(\frac{\text{Re}[\sigma(\Omega)] - 1/4}{\omega - \Omega} \right), \end{aligned} \quad (3.5)$$

where \mathcal{P} is the principal part. Note that this reduces to Eq. (2.34) in the limit $\omega \gg T$. However, the most important new feature of Eq. (3.5) arises for $\omega \ll T$, where we find a delta function at zero frequency in the real part. Thus the d.c. conductivity is infinite at this order, arising from the collisionless transport of thermally excited carriers.

Exercise: Evaluate K_{00} from Eq. (2.31) at $T > 0$. First perform the trace over the Dirac matrices, and then the summation over the frequency. Subtract from your answer the result of integrating over the frequency; this subtraction can be compensated by the $T = 0$ result in Eq. (2.31). The remaining expressions are explicitly convergent in the ultraviolet, and the integration over spatial momenta can be evaluated. Finally, analytically continue the answer to real frequencies to obtain Eq. (3.5).

The relaxational processes associated with Eq. (3.4) should lead to collisions between the thermally excited carriers and broaden the delta function at zero frequency. However, this relaxation does appear in a direct perturbative analysis of the critical theory in powers of $(3 - d)$ or $1/N$. As has been discussed elsewhere²⁵⁻³¹, an infinite order resummation is required, whose simplest realization requires solution of a quantum Boltzmann equation. Such a solution shows that the delta function acquires a width of order $(3 - d)^2 T$ or T/N , and so there is a large d.c. conductivity of order $(3 - d)^{-2}$ or N . Thus $\sigma(\omega)$ has the form of ‘Drude peak’ at zero frequency, and the behavior in Eq. (2.35) for $\omega \gg T$. However, the accuracy of such a Boltzmann equation computation is untested, and it is likely that such perturbative analyses of quantum-critical dynamics are quantitatively unreliable.

We will be satisfied here by scaling arguments which generalize the $T = 0$ quantum-critical results in Eq. (2.35) to the $T > 0$ quantum critical region in Fig. 6. The quantum-critical relaxational processes invalidate the form in Eq. (2.35) for the density correlation function, and we instead expect the form dictated by the hydrodynamic diffusion of charge. Thus for K_{00} , Eq. (2.35) applies only for $\omega \gg T$, while

$$K_{00}(\omega, k) = \chi \frac{Dk^2}{Dk^2 - i\omega} \quad , \quad \omega \ll T. \quad (3.6)$$

Here χ is the charge susceptibility (here it is the compressibility), and D is the charge diffusion constant. Associated with Eq. (3.4), these have universal values in the quantum critical region:

$$\chi = \mathcal{C}_\chi T \quad , \quad D = \frac{\mathcal{C}_D}{T}, \quad (3.7)$$

where again \mathcal{C}_χ and \mathcal{C}_D are universal numbers. For the conductivity, we expect a crossover from the collisionless critical dynamics at frequencies $\omega \gg T$, to a hydrodynamic collision-dominated form for $\omega \ll T$. This entire crossover is universal, and is described by a universal crossover function

$$\sigma(\omega) = \mathcal{K}_\sigma(\omega/T). \quad (3.8)$$

The result in Eq. (2.35) applies for $\omega \gg T$, and so

$$\mathcal{K}_\sigma(\infty) = \mathcal{K}. \quad (3.9)$$

For the hydrodynamic transport, we apply the Kubo formula in Eq. (2.33) to Eq. (3.6) and obtain

$$\mathcal{K}_\sigma(0) = \mathcal{C}_\chi \mathcal{C}_D \quad (3.10)$$

which is a version of Einstein’s relation for Brownian motion.

B. The AdS/CFT correspondence

Portions of this section have been adapted from Chapter 15 of Ref. 19.

It turns out the AdS/CFT correspondence is ‘just what the doctor ordered’ to compute strongly-coupled quantum critical dynamics and transport in the orange-colored region of Fig. 6. This is a consequence of a crucial property: even at the level of the classical gravity approximation in the AdS theory, the system relaxes back to thermal equilibrium in a time which obeys Eq. (3.4). No other method in condensed matter physics shares this remarkable feature. We will review specific computations by this method of the universal function $\mathcal{K}_\sigma(\omega/T)$, and of the collisionless-to -hydrodynamic crossover in the density correlation function.

The CFT solvable by the AdS/CFT correspondence may be viewed as a generalization of the CFT described by Eq. (2.27). It has a closer resemblance to the SU(2) gauge theory we consider later in Eq. (5.8). We take the structure of critical matter fields coupled to a gauge field, and generalize it to a relativistically invariant model with a non-Abelian SU(N) gauge group and the maximal possible supersymmetry. The resulting supersymmetric Yang-Mills (SYM) theory has only one independent coupling constant g . Under the RG, it is believed that g flows to an attractive fixed point at a non-zero coupling $g = g^*$; the fixed point then defines a supersymmetric conformal field theory in 2+1 dimensions (a SCFT3). We are interested here in computing the transport properties of the SCFT, as a paradigm of quantum critical transport at a strongly interacting quantum critical point.

The solution proceeds by a dual formulation as a four-dimensional supergravity theory on a spacetime with uniform negative curvature: anti-de Sitter space, or AdS₄. The solution is also easily extended to non-zero temperatures, and allows direct computation of the correlators of conserved charges in real time. At $T > 0$ a black hole appears in the gravity theory, resulting in an AdS-Schwarzschild spacetime, and T is the Hawking temperature of the black hole; the real time solutions also extend to $T > 0$.

The reader is referred to the original paper³², and to the TASI lectures by Son for an explicit description of the method. In the AdS/CFT correspondence, every globally conserved quantity in the CFT gets mapped onto a gauge field in AdS. Moreover, in the leading classical gravity theory on AdS, different global charges commute with each other, and so can be considered separately. In the end, we have a U(1) gauge field on AdS for every global conservation law of the CFT. The low energy effective field theory on AdS₄ has the standard Einstein-Maxwell action for gravity+electromagnetism:

$$\mathcal{S}_M = \frac{1}{g_4^2} \int d^4x \sqrt{-g} \left[-\frac{1}{4} F_{ab} F^{ab} \right]. \quad (3.11)$$

Here g_{ab} is the AdS-Schwarzschild metric (g is its determinant), F_{ab} is the Maxwell flux tensor, and g_4 is a dimensionless coupling constant fixed by the value of N in the SU(N) SYM

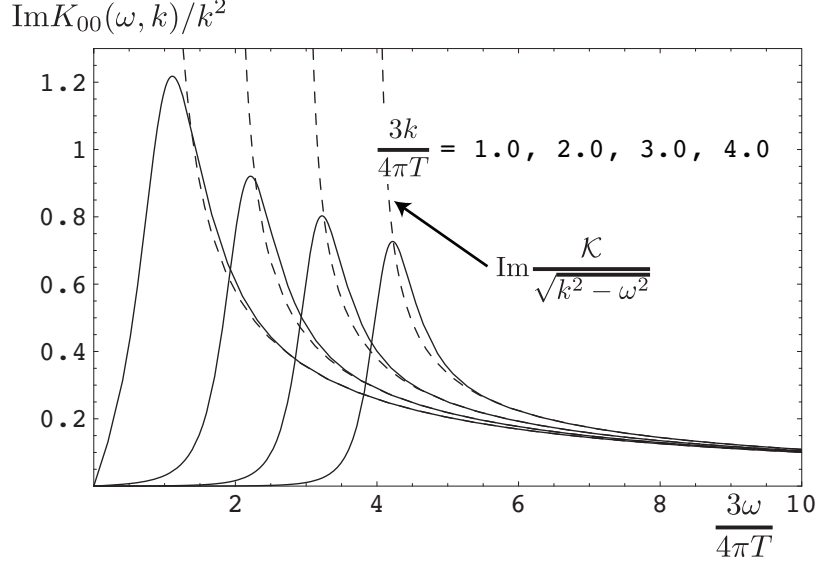


FIG. 7: Spectral weight of the density correlation function of the SCFT3 with $\mathcal{N} = 8$ supersymmetry in the collisionless regime

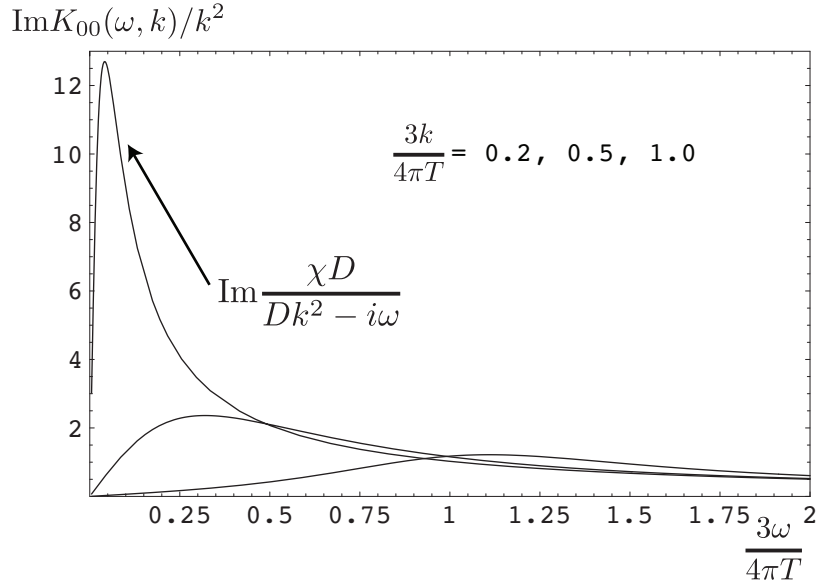


FIG. 8: As in Fig. 7, but for the collision-dominated regime.

theory. This 4-dimensional Maxwell theory can be used to compute the density correlation function, $K_{00}(\omega, k)$, of the 3-dimensional SYM theory, and the results are shown in Fig. 7 and 8. The most important feature of these results is that the expected limiting forms in the collisionless (Eq. (2.35)) and collision-dominated (Eq. (3.6)) are obeyed. Thus the results do display the collisionless to collision-dominated crossover at a frequency of order $k_B T/\hbar$, as we expected from the physical discussion in Section III A.

At this point, we describe some technical aspects of the results which turn out to have important physical implications. For this, let us generalize the constraints on $K_{\mu\nu}$ from

current conservation in Eq. (2.32) to non-zero temperatures. At $T > 0$, we do not expect $K_{\mu\nu}$ to be relativistically covariant, and so can only constrain it by spatial isotropy and density conservation. These two constraints, along with dimensional analyses, lead to the most general form

$$K_{\mu\nu}(\omega, \mathbf{k}) = \sqrt{k^2 - \omega^2} \left(P_{\mu\nu}^T K^T(\omega, k) + P_{\mu\nu}^L K^L(\omega, k) \right), \quad (3.12)$$

where $p_\mu \equiv (-\omega, \mathbf{k})$ and $k = |\mathbf{k}|$. The $K^{L,T}$ are dimensionless functions of the arguments, and depend upon ω and the magnitude of the 2-vector \mathbf{k} . Also $P_{\mu\nu}^T$ and $P_{\mu\nu}^L$ are orthogonal projectors defined by

$$P_{00}^T = P_{0i}^T = P_{i0}^T = 0 \quad , \quad P_{ij}^T = \delta_{ij} - \frac{k_i k_j}{k^2} \quad , \quad P_{\mu\nu}^L = \left(\eta_{\mu\nu} - \frac{k_\mu k_\nu}{p^2} \right) - P_{\mu\nu}^T, \quad (3.13)$$

with $\eta_{\mu\nu} = \text{diag}(-1, 1, 1)$, and the indices i, j running over the 2 spatial components. Thus, in the general case at $T > 0$, the full density and current responses are described in terms of two functions $K^{L,T}(k, \omega)$, representing current fluctuations longitudinal and transverse to the momentum. These two functions are not entirely independent. At $T > 0$, we expect all correlations to be smooth functions at $k = 0$: this is because all correlations are expected to decay exponentially to zero as a function of spatial separation. However, this is only possible from (3.12) if we have the additional relation

$$K^T(\omega, 0) = K^L(\omega, 0). \quad (3.14)$$

Finally, we note that application of the Kubo formula in Eq. (2.33) to Eq. (3.12) yields

$$\sigma(\omega) = K^L(\omega, 0). \quad (3.15)$$

The relations of the previous paragraph are completely general and apply to any theory. Specializing to the AdS-Schwarzschild solution of SYM3 as determined by the Einstein-Maxwell theory in Eq. (3.11), the results were found to obey a simple and remarkable identity³²:

$$K^L(\omega, k) K^T(\omega, k) = \mathcal{K}^2 \quad (3.16)$$

where \mathcal{K} is a known pure number, independent of ω and k . This identity is a consequence of the self-dual structure of Eq. (3.11): the Maxwell action in 3+1 dimensions is well-known to have a self-dual structure corresponding to the exchange of electric and magnetic fields. Thus we have the important and key result that every global charge in a CFT3 maps onto a self-dual theory in the leading gravity approximation on AdS₄. The identity in (3.16) is a consequence of this emergent self-duality of CFT3s.

The combination of (3.16) and (3.14) now fully determine the response functions at zero momenta: $K^L(\omega, 0) = K^T(\omega, 0) = \mathcal{K}$. Computing the conductivity from Eq. (3.15), we then

have

$$\sigma(\omega) = \mathcal{K}_\sigma(\omega/T) = \mathcal{K}; \quad (3.17)$$

i.e. the scaling function in Eq. (3.8) is *independent* of ω and equal to the value in Eq. (3.9). This result is an important surprise: the conductivity of the classical gravity theory on AdS₄ is frequency-independent. Furthermore, its value is fixed by self-duality to be the constant \mathcal{K} appearing in the self-duality relation (3.16). All these remarkable results are a direct consequence of the self-duality of the U(1) Maxwell theory on AdS₄.

Given the strong consequences of self-duality relation in Eq. (3.16), it is useful to ask whether it can be valid for CFTs beyond those described by the classical Einstein-Maxwell theory on AdS₄. This question was addressed recently by Myers *et al.*³³. They examined the general structure of the higher-derivative corrections to Eq. (3.11), and argued that for the current correlations the leading terms could always be transformed into the following form which has only *one* dimensionless constant γ (L is the radius of AdS₄):

$$\mathcal{S}'_M = \frac{1}{g_4^2} \int d^4x \sqrt{-g} \left[-\frac{1}{4} F_{ab} F^{ab} + \gamma L^2 C_{abcd} F^{ab} F^{cd} \right], \quad (3.18)$$

where the extra four-derivative interaction is expressed in terms of the Weyl tensor C_{abcd} . A crucial observation of Ref. 33 was that stability and causality constraints on the effective theory restrict $|\gamma| < 1/12$. A generalized duality relation applies also to \mathcal{S}'_M . However this is *not* a *self*-duality. The dual CFT has current correlation functions which were characterized by functions $\tilde{K}^{L,T}(\omega, k)$ which are distinct from those of the direct CFT $K^{L,T}(\omega, k)$, and the self-duality relation of Eq. (3.16) take the less restrictive form

$$K^L(\omega, k) \tilde{K}^T(\omega, k) = \mathcal{K}^2 \quad , \quad K^T(\omega, k) \tilde{K}^L(\omega, k) = \mathcal{K}^2. \quad (3.19)$$

These duality relation determines the correlators of the dual CFT in terms of the direct CFT, but do not fix the latter. Determination of the functions $K^L(\omega, 0) = K^T(\omega, 0)$ requires explicit computation using the extended theory \mathcal{S}_{vec} , and the results for the conductivity are presented in Fig. 9. Now the conductivity does have a non-trivial universal dependence on ω/T . However, as is clear from Fig, 9, stability conditions on the effective theory on AdS₄ allow only a limited range of dependence on ω/T . The smooth ω/T dependence in Fig. 9 should be contrasted to the very singular dependence in the free-field result in Eq. (3.5); the former is clearly more generic for a strongly-coupled CFT. It is also interesting to note that the ω/T dependence in Fig. 9 for $\gamma > 0$ is very similar to the structure we discussed in Section III A on the effect of collisional broadening of the singularities in Eq. (3.5): the AdS₄ result shows a collision-dominated Drude peak at $\omega = 0$, and a collisionless critical continuum at large ω .

Does the duality mapping of Myers *et al.*³³ have an interpretation directly in the CFT, without using the mapping to AdS₄? It has been argued³²⁻³⁴ that this duality is the analog

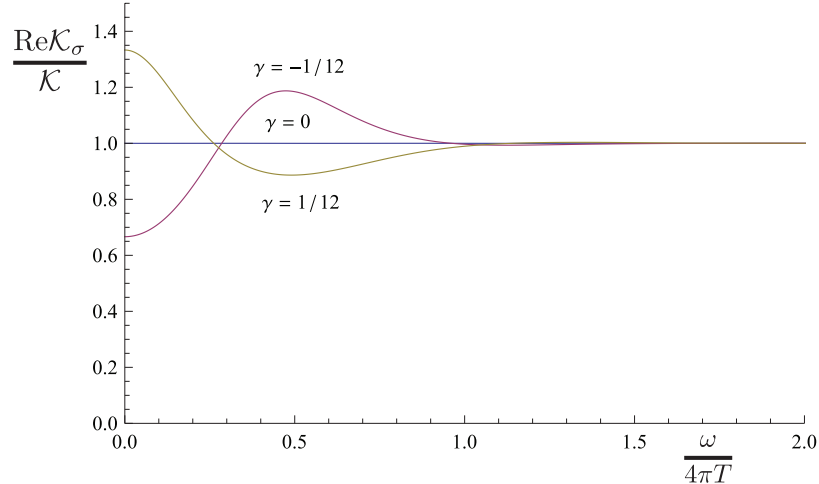


FIG. 9: Frequency dependent conductivity for CFT3s for which the AdS₄ theory includes the leading correction beyond the Einstein-Maxwell theory from Ref. 33. The co-efficient of this correction in the action is γ , and stability requirements impose the bound $|\gamma| < 1/12$.

of the ‘particle-vortex’ duality of condensed matter physics. The latter is an exact duality of the critical theory of a complex relativistic scalar field³⁵ (this the theory in Eq. (2.27) without the fermions, and with φ^a having two components). In the particle-vortex duality, the world line of the complex scalars is reinterpreted as the world line of vortices in the dual theory of a dual complex scalar interacting with an emergent electromagnetic field. This particle-vortex duality also allows us to interpret the structure of the results in Fig. 9 for $\gamma < 0$. Note that from Eq. (3.19) the conductivity of the direct CFT maps onto the resistivity of the dual CFT. Thus for $\gamma < 0$, it is the dual CFT which will have a conductivity which has the structure discussed in Section III A, with a collisionally-broadened Drude peak at $\omega = 0$. Thus we conclude that a Boltzmann-like picture of transport applies better to the particle interpretation of the CFT for $\gamma > 0$, and to the vortex interpretation for $\gamma < 0$.

Let us summarize the lessons we have learnt from the AdS theory of quantum critical transport in strongly interacting systems in 2+1 dimensions. This theory should be view as complementary to the quasiparticle-based theory, whose implications were discussed in Section III A. The lessons are:

- There are a large class of strongly interacting 2+1 dimensional quantum liquids which relax back to thermal equilibrium in the shortest possible time of order $\hbar/(k_B T)$, as we indicated in (3.4).
- The quasiparticle transport theory^{25–31} starts from the free theory with an infinite thermal equilibration time, and includes the effect of weak interactions using the Boltzmann equation. Complementary to this is the quantum-critical transport theory applicable for the shortest possible equilibration time of order $\hbar/(k_B T)$, which is the classical Einstein-Maxwell theory on AdS₄.

- The Einstein-Maxwell theory exhibits collisionless dynamics for $\omega \gg T$, and collision-dominated dynamics for $\omega \ll T$, as we displayed in Figs. 7 and 8.
- All continuous global symmetries are represented by a self-dual Einstein-Maxwell theory.
- This emergent self-duality implies that, in systems with particle-hole symmetry, $\sigma(\omega)$ is frequency-independent in the Einstein-Maxwell theory and equal to the self-dual value.
- For systems with particle-hole symmetry, a frequency dependent conductivity is obtained³³ upon considering corrections to the effective Einstein-Maxwell theory, with the forms in Fig. 9. Stability conditions on the effective theory allow only a limited range of frequency dependence, which depend upon the single parameter $|\gamma| < 1/12$. For $\gamma > 0$, the frequency dependence has the form expected from collision-dominated transport of particles, while for $\gamma < 0$ it is characteristic of the transport of vortices. It is remarkable that the physical pictures expected from the Boltzmann transport analysis correspond to precisely those obtained from the holographic approach.
- Such quantum-critical fluids also have universal momentum transport. By extending the scaling arguments to momentum transport we would conclude that the ratio of the shear viscosity to the entropy density η/s should equal a universal number characterizing the collision-dominated regime. This number was computed in the Einstein-Maxwell theory by Kovtun *et al.*^{36,37} and found to equal $\hbar/(4\pi k_B)$. The shortest possible relaxation time implies that η is also the smallest possible and so these fluids are ‘nearly perfect’.

IV. U(1) GAUGE THEORY AND THE VALENCE BOND SOLID ON THE HONEYCOMB LATTICE

We now return to the honeycomb lattice at half-filling. In Section IID we described a quantum phase transition in which two characteristics of the ground state changed simultaneously. In the charge sector, the one electron excitation gap opened up leading to a transition from the semi-metal to the insulator. And in the spin sector, the breaking of SU(2) spin rotation symmetry led to Néel order in the insulator. However, in the Mott picture, the insulating behavior is tied to repulsion between the electrons, which keeps them apart, rather than to any specific symmetry breaking. This would suggest that it is possible to have an insulating state while preserving spin rotation invariance. We will explore such a possibility in the present section.

Readers not interested in issues related to electron fractionalization and emergent gauge fields in insulators may skip ahead to the discussion of metallic phases in Section VI.

Our approach will begin in the Néel-ordered insulator, and restore spin rotation invariance by allowing for slow angular fluctuations in the local *orientation* of the Néel order parameter φ^a . At the same time, it will also pay to transform the fermions to a ‘rotating reference frame’ so that their spin is measured relative to the orientation of the local Néel order^{38–40}. This transformation is most conveniently done using spinor variables. So let us decompose the vector Néel order φ^a into a complex two-component bosonic spinor z_α by

$$\varphi^a = z_\alpha^* \sigma_{\alpha\beta}^a z_\beta \quad (4.1)$$

Such a decomposition is familiar from early work of D’Adda *et al.*⁴¹ and Witten⁴², who established the equivalence between the O(3) non-linear σ -model and the CP¹ model in 2 spacetime dimensions. A similar equivalence does not immediately apply in the 3 spacetime dimensional case of interest here because point defects in spacetime have to be treated with some care⁴³. In particular, the theory for the fluctuations of the vector field φ^a must allow for point spacetime defects (‘instantons’) where $\varphi^a = 0$, which are known in the condensed matter literature as ‘hedgehogs’. Note that these hedgehogs are present even in a ‘fixed-length’, non-linear σ -model in which we set $\varphi^{a2} = 1$; such models require ultraviolet regularization, and the hedgehogs are invariably permitted in the regulated theory *e.g.* with a lattice regularization. Ignoring these defects momentarily, let us proceed as in the earlier work^{41,42}. The parameterization in Eq. (4.1) is invariant under the U(1) gauge transformation

$$z_\alpha \rightarrow z_\alpha e^{i\zeta} \quad (4.2)$$

and so the theory for the z_α must be a U(1) gauge theory involving an emergent U(1) gauge field A_μ . The boson only terms in Eq. (2.27) are equivalent^{41,42} to a U(1) gauge theory for the complex scalars z_α

$$\mathcal{L}_z = |(\partial_\mu - iA_\mu)z_\alpha|^2 + s|z_\alpha|^2 + u(|z_\alpha|^2)^2. \quad (4.3)$$

Here the gauge field A_μ is dynamical, and will acquire a Maxwell action after high energy z_α modes have been integrated out.

Let us now discuss the point defects. Eqn (4.1) implies⁴³ that the hedgehogs in φ^a become Dirac monopoles in A_μ : these are tunnelling events associated with a change in the total A_μ flux by 2π . Such monopoles are permitted by the U(1) gauge theory in Eq. (4.3) only if the U(1) gauge field is *compact*. So we must account for the dynamics of such a compact U(1) gauge theory to completely account for the fluctuations of the local antiferromagnetic order. The dynamics of the matter fields can suppress the monopoles in some cases^{44–46}, and this can then lead to deconfined critical points or phases with a gapless U(1) photon excitation associated with an effectively non-compact U(1) gauge field. We will find an example of this phenomenon in Section VII.

Let us now turn to the fermionic excitations in antiferromagnetic insulator. We transform these to the rotating reference frame by writing^{38–40}

$$\begin{pmatrix} c_\uparrow \\ c_\downarrow \end{pmatrix} = \begin{pmatrix} z_\uparrow & -z_\downarrow^* \\ z_\downarrow & z_\uparrow^* \end{pmatrix} \begin{pmatrix} \psi_+ \\ \psi_- \end{pmatrix} \quad (4.4)$$

where ψ_p , $p = \pm$, are the “electrons” in the rotating reference frame. The index p measures the spin-projection along the direction of the local Néel order. However, more properly it is the “charge” under the emergent U(1) gauge field because Eq. (4.4) is invariant under Eq. (4.2) and

$$\psi_+ \rightarrow \psi_+ e^{-i\zeta} \quad , \quad \psi_- \rightarrow \psi_- e^{i\zeta}. \quad (4.5)$$

An important consequence of Eqs. (4.4) and (4.1) is the identity

$$\varphi^a c_\alpha^\dagger \sigma_{\alpha\beta}^a c_\beta = (|z_\alpha|^2)^2 \left(\psi_+^\dagger \psi_+ - \psi_-^\dagger \psi_- \right). \quad (4.6)$$

Thus the effective moment acting on the ψ fermions is always along the z axis, as expected by the transformation to a rotating reference frame.

Let us now take the continuum limit for the fermions in the rotating reference frame. We follow exactly the same mapping as in Eq. (2.8) to map the lattice ψ fermions to continuum 8-component Ψ fermions. Based upon Eq. (4.6), we also expect the Ψ fermions to experience a field polarized along the σ^z direction. Combined with gauge invariance, and the structure of Eq. (2.27), we are led to the following Lagrangian density for Ψ :

$$\mathcal{L}_\Psi = \bar{\Psi} \gamma_\mu (\partial_\mu + i\sigma^z A_\mu) \Psi - \lambda N_0 \bar{\Psi} \rho^z \sigma^z \Psi. \quad (4.7)$$

Note this is the theory of Dirac fermions of mass $|\lambda N_0|$ coupled to a U(1) gauge field. The coupling of the fermions to the U(1) gauge field in Eq. (4.7) can also be derived explicitly by substituting Eq. (4.4) into the last term in Eq. (2.27), and using the expression for the U(1) gauge field in the CP¹ model. We will present a more explicit derivation of an emergent gauge field for the case of the triangular lattice in Section VI below.

The Lagrangian $\mathcal{L}_z + \mathcal{L}_\Psi$ is then our U(1) gauge theory for the fluctuating Néel state, complementary to the Gross-Neveu-Yukawa theory in Eq. (2.27). The remainder of this section is devoted to understanding the physical properties of $\mathcal{L}_z + \mathcal{L}_\Psi$.

Let us now discuss the phases of this U(1) gauge theory.

First, we have the Higgs phase, where $s < 0$ and z_α is condensed. Here the U(1) photon is gapped, and spin rotation invariance is broken. This is just the insulating Néel state, and its properties are identical to the Néel ordered state described by Eq. (2.27).

The other phase with $s > 0$ has z_α gapped and spin rotation invariance is preserved. However, as is clear from Eq. (4.7), the fermionic spectrum remains gapped. Thus this phase is clearly not the semi-metal of Eq. (2.27). Instead it is a new insulating phase with

spin rotation invariance preserved. Thus we have achieved our objective of describing an insulator without Néel order.

However, this insulator is not a featureless state with a spin and a charge gap, as we will now show. The interesting physics arises from an interplay of the monopole events with the filled band of fermionic states. If we integrate out this filled band via \mathcal{L}_Ψ , we generate an effective Maxwell action for the U(1) gauge field

$$\mathcal{L}_A = \frac{1}{12\pi|\lambda N_0|}(\epsilon_{\mu\nu\lambda}\partial_\nu A_\lambda)^2 \quad (4.8)$$

We recall that the U(1) gauge field is compact, and it was shown by Polyakov⁴⁷ that such a gauge field always acquires a mass gap and is in a confining phase in 2+1 dimensions. The confinement is caused by the proliferation of monopole tunneling events. Here we will show^{13,43,46,48} that the monopole operator has non-trivial transformation properties under the symmetry group of the honeycomb lattice: consequently, the proliferation of monopoles in the confining phase breaks a lattice symmetry due to the appearance of valence bond solid (VBS) order.

To see this, it is useful to add an external source B_μ to the fermion Lagrangian in Eq. (4.7) so that \mathcal{L}_Ψ becomes

$$\mathcal{L}_\Psi = \bar{\Psi}\gamma_\mu(\partial_\mu + i\sigma^z A_\mu)\Psi - \lambda N_0 \bar{\Psi}\rho^z\sigma^z\Psi - \frac{i}{2}B_\mu\bar{\Psi}\gamma_\mu\rho^z\Psi. \quad (4.9)$$

This source has been judiciously chosen so that when we integrate out the fermions, the action for the A_μ gauge field in Eq. (4.8) acquires a mutual Chern-Simons term^{13,48}

$$\mathcal{L}_A = \frac{1}{12\pi|\lambda N_0|}(\epsilon_{\mu\nu\lambda}\partial_\nu A_\lambda)^2 + \frac{i}{2\pi}B_\mu\epsilon_{\mu\nu\lambda}\partial_\nu A_\lambda \quad (4.10)$$

Let us now proceed with Polyakov's duality mapping on Eq. (4.10) to obtain an effective theory of monopoles: the B_μ source term will allow us to deduce the connection between the monopole operator and the underlying lattice fermions. The first step corresponds to decoupling the Maxwell term by a Hubbard-Stratonovich field, Y_μ , to obtain

$$\mathcal{L}_A = \frac{3|\lambda N_0|}{4\pi}Y_\mu^2 + \frac{i}{2\pi}Y_\mu\epsilon_{\mu\nu\lambda}\partial_\nu A_\lambda + \frac{i}{2\pi}B_\mu\epsilon_{\mu\nu\lambda}\partial_\nu A_\lambda \quad (4.11)$$

Now, we integrate over A_μ , and this yields the constraint

$$Y_\mu = \partial_\mu\phi - B_\mu. \quad (4.12)$$

where ϕ is the scalar field which is dual to the photon. We have judiciously chosen factors of (2π) above to ensure a normalization so that $e^{i\phi}$ is the monopole operator. Finally, inserting

Eq. (4.12) into (4.11) we obtain^{13,48}

$$\mathcal{L}_\phi = \frac{3|\lambda N_0|}{4\pi}(\partial_\mu\phi - B_\mu)^2. \quad (4.13)$$

In the absence of the external source B_μ this is a free scalar field theory, which implies that the monopole operator $e^{i\phi}$ has long-range correlations in 2+1 dimensions. In other words, the free photon phase described by Eq. (4.8) has a non-zero VEV with $\langle e^{i\phi} \rangle \neq 0$.

The B_μ term in Eq. (4.13) will help us link the monopole operator to the underlying electrons⁴⁸. First, we notice that the theory in Eq. (4.9) actually enjoys a gauge invariance under which

$$\Psi \rightarrow \exp\left(i\frac{\rho^z}{2}\theta\right)\Psi \quad , \quad B_\mu \rightarrow B_\mu - \partial_\mu\theta \quad (4.14)$$

where θ is a field with an arbitrary spacetime dependence. (Note that this gauge invariance is distinct from that associated with the A_μ gauge field in Eq. (4.5), under which $\Psi \rightarrow \exp(-i\sigma^z\zeta)\Psi$.) Now we observe that this gauge invariance extends also to Eq. (4.13), under which

$$e^{i\phi} \rightarrow e^{i\theta}e^{i\phi}. \quad (4.15)$$

The combination of Eqs. (4.14) and (4.15) now allows us to identify the operator $e^{i\phi}$. We look for a fermion bilinear of the form $\bar{\Psi}M\Psi$ so it transforms like Eq. (4.15) under the gauge transformation in Eq. (4.14). Moreover, the Lorentz invariance of the theory implies that the matrix M should commute with the γ_μ matrices in Eq. (2.12). This leads us to the unique choice

$$e^{i\phi} \sim \bar{\Psi}\tau^y(\rho^x + i\rho^y)\Psi \sim \bar{C}\tau^y(\rho^x + i\rho^y)C \quad (4.16)$$

It now remains to use the geometric definitions in Section II A and Eq. (2.8) to deduce the physical interpretation of the fermion bilinear in Eq. (4.16). A careful analysis⁴⁸ along these lines shows that $e^{i\phi}$ is an operator associated with the valence bond solid (VBS) order in Fig. 10, and the VEVs of the operators in Eq. (4.16) imply long-range VBS order.

Exercise: Compute the transformations of the fermion bilinear in Eq. (4.16) under honeycomb lattice symmetries such as translations, reflections, and rotations by 60 degrees. All these transformations map the pattern in Fig. 10 either to itself or to 2 equivalent patterns. Assign the weights 1, $e^{2\pi i/3}$, and $e^{4\pi i/3}$ to these patterns, and show that their transformations coincide with those of Eq. (4.16).

Thus we reach our main conclusion: the insulating phase without Néel order as described by the U(1) gauge theory $\mathcal{L}_z + \mathcal{L}_\Psi$ has long-range VBS order. This order onsets with the confinement induced by the proliferation of monopoles.

It is interesting to note that the matrices in the fermion bilinears associated with VBS

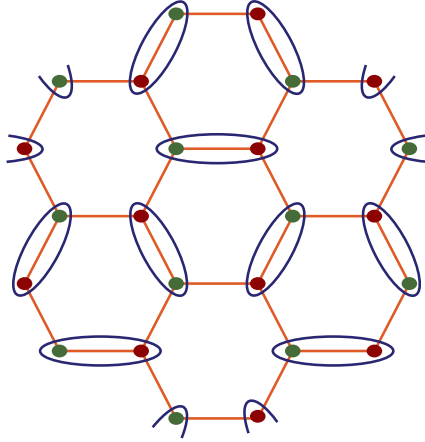


FIG. 10: A schematic illustration of the valence bond solid (VBS). The ellipses represent singlet valence bonds between the electrons. These reside preferentially in the pattern shown in the VBS state. Expectation values of all spin-singlet observables, such as $S_i^a S_j^a$ or $c_{i\alpha}^\dagger c_{j\alpha} + c_{j\alpha}^\dagger c_{i\alpha}$, are different on the links with the ellipses than those without.

order $\sim \bar{C}\tau^y(\rho^x + i\rho^y)C$ and Néel order $\sim \bar{C}\rho^z\sigma^a C$ all anti-commute with each other, and commute with the γ_μ matrices in Eq. (2.12). This can be used to formulate the present theory without gauge fields but using a Wess-Zumino-Witten term^{48–52}: we will not explore this approach here.

We can also use the methods of this section to address the nature of the transition between the Néel and VBS phases. We will not go into details here, but this transition has been proposed^{45,46} to be a deconfined critical point at which monopoles are suppressed, and the critical theory is the non-compact version of the U(1) gauge theory given by \mathcal{L}_z .

V. SU(2) GAUGE THEORY AND A PHASE DIAGRAM FOR THE HALF-FILLED HONEYCOMB LATTICE

Sections II and IV have so far described 3 possible phases of the honeycomb lattice at half-filling: the semi-metal, the insulator with Néel order, and the insulator with VBS order. The first two phases appear in the theory \mathcal{L} in Eq. (2.27), while the latter two appear in the theory $\mathcal{L}_z + \mathcal{L}_\Psi$ in Eqs. (4.3) and (4.7). This is an unsatisfactory state of affairs: we would like to write down a single unified theory in which all 3 phases appear. One approach, implicitly mentioned above, is to extend Eq. (2.27) by including an additional two-component real scalar field representing the VBS order parameter, and couple it to the fermion bilinear $\bar{C}\tau^y(\rho^x + i\rho^y)C$ appearing in Eq. (4.16). Integrating out the fermions in the background of a spatially varying 5-component scalar representing the Néel and VBS orders yields a Wess-Zumino-Witten term for the scalar field^{48–52}. The resulting theory is difficult to work with, and little is known about it in the regime where all three phases can meet.

Here we will present an alternative approach which allows for exotic phases using an

emergent SU(2) gauge field. We will find that the resulting phase diagram has a fourth semi-metallic phase with an emergent topological order, and an interesting multicritical point.

Our starting point is the observation that the decomposition of the electron into spinful bosons and spinless charged fermions in Eq. (4.4) has a larger gauge invariance⁴⁰ than U(1). Rewriting eq. (4.4) using a natural matrix notation

$$c = R\psi \quad (5.1)$$

where

$$R \equiv \begin{pmatrix} z_{\uparrow} & -z_{\downarrow}^* \\ z_{\downarrow} & z_{\uparrow}^* \end{pmatrix}, \quad (5.2)$$

we note that Eq. (5.1) is invariant under the gauge transformation generated by SU(2)_g matrix U under which

$$R \rightarrow RU^{\dagger} \quad , \quad \psi \rightarrow U\psi \quad , \quad c \rightarrow c. \quad (5.3)$$

This SU(2)_g gauge transformation should be distinguished from the global SU(2) spin rotation V , under which

$$R \rightarrow VR \quad , \quad \psi \rightarrow \psi \quad , \quad c \rightarrow Vc. \quad (5.4)$$

Turning to the Néel order φ^a , this clearly transforms as a **3** under the global SU(2). However, the parameterization for the Néel order in Eq. (4.1) is not invariant the SU(2)_g gauge transformation in Eq. (5.3). As written, Eq. (4.1) is invariant only under the U(1) gauge transformation in Eq. (4.2) which was the reason for our original choice of a U(1) gauge theory in Section IV. Thus we cannot use Eq. (4.1) as our definition of the Néel order in the present SU(2) gauge theory.

It is more natural to proceed here^{13,40} by defining the scalar fields using bilinears of the fermions. Thus using Eq. (2.25) and extending to continuum 8-component fermions near the Fermi points, we define

$$\varphi^a = \bar{C}\rho^z\sigma^a C. \quad (5.5)$$

From this definition it is clear that φ^a transforms as a **3** under the global SU(2), while it is invariant under SU(2)_g, just as expected.

We can also define the corresponding scalar using the ψ fermions⁴⁰:

$$\Phi^a = \bar{\Psi}\rho^z\sigma^a\Psi. \quad (5.6)$$

Now Φ^a transforms as a **3** under the gauge SU(2)_g, while it is invariant under SU(2).

From Eqs. (5.1), (5.5) and (5.6), we find that the scalar fields are related by

$$\begin{aligned}\varphi^a &= \frac{1}{2}\Phi^b \text{Tr}(\sigma^a R \sigma^b R^\dagger) \\ \Phi^a &= \frac{1}{2}\varphi^b \text{Tr}(\sigma^b R \sigma^a R^\dagger) (|z_\alpha|^2)^2.\end{aligned}\tag{5.7}$$

These relations generalize Eq. (4.1) from the U(1) gauge theory.

To summarize, the matter fields of our $SU(2)_g$ gauge theory are the bosonic matrix R , the fermions Ψ , and the scalar Φ^a . As in Section IV, we will also need an emergent dynamic $SU(2)_g$ gauge field A_μ^a . Using symmetry and gauge invariance, we can now write down the following Lagrangian density⁴⁰ for the SU_g gauge theory; this combines and generalizes the Gross-Neveu-Yukawa model in Eq. (2.27), and the U(1) gauge theory in Eqs. (4.3) and (4.7).

$$\begin{aligned}\mathcal{L}_g &= \bar{\Psi}\gamma_\mu(\partial_\mu + i\sigma^a A_\mu^a)\Psi - \lambda\Phi^a\bar{\Psi}\rho^z\sigma^a\Psi \\ &+ \frac{1}{2}\left[(\partial_\mu\Phi^a - 2\epsilon_{abc}A_\mu^b\Phi^c)^2 + s\Phi^{a2}\right] + \frac{u}{24}(\Phi^{a2})^2 \\ &+ \text{Tr}\left[(\partial_\mu R - iA_\mu^a R\sigma^a)(\partial_\mu R^\dagger + iA_\mu^a\sigma^a R^\dagger)\right] \\ &+ \tilde{s}\text{Tr}(RR^\dagger) + \tilde{u}\left[\text{Tr}(RR^\dagger)\right]^2.\end{aligned}\tag{5.8}$$

This Lagrangian combines all three phases discussed so far, and forms the basis of our remaining discussion of the honeycomb lattice at half-filling.

In mean-field theory, the model \mathcal{L}_g has 4 phases, depending upon whether one or both of the scalar fields Φ^a and R are condensed. These 4 phases can be identified using the methods developed in Section IID and IV, and lead to the phase diagram shown in Fig. 11. First, we describe how \mathcal{L}_g reproduces the phases and phase transitions already discussed:

- The Higgs phase where $\langle R \rangle \neq 0$ breaks $SU(2)_g$ completely. Using $SU(2)_g$ gauge invariance we may as well set $R = 1$. Then from Eq. (5.7), we have $\Phi^a \sim \varphi^a$, the Néel order parameter. Also the gauge boson A_μ^a is gapped and can be neglected. Then the theory \mathcal{L}_g reduces to the Gross-Neveu-Yukawa model in Eq. (2.27). As discussed in Section IID, this theory has semi-metal and insulating Néel phases, and these are shown in Fig. 11.
- The Higgs phase where $\langle N^a \rangle \neq 0$ breaks $SU(2)_g$ down to U(1). Then only the A_μ^z (say) gauge boson is active, and the theory \mathcal{L}_g reduces to the U(1) gauge theory $\mathcal{L}_z + \mathcal{L}_\Psi$ discussed in Section IV. The insulating Néel and insulating VBS phases found there are also shown in Fig. 11.

The possible new phase of \mathcal{L}_g is the deconfined phase where both Φ^a and R are gapped. Then the low energy theory of \mathcal{L}_g is simply massless QCD with the Lagrangian density

$$\mathcal{L}_{QCD} = \bar{\Psi}\gamma_\mu(\partial_\mu + i\sigma^a A_\mu^a)\Psi.\tag{5.9}$$

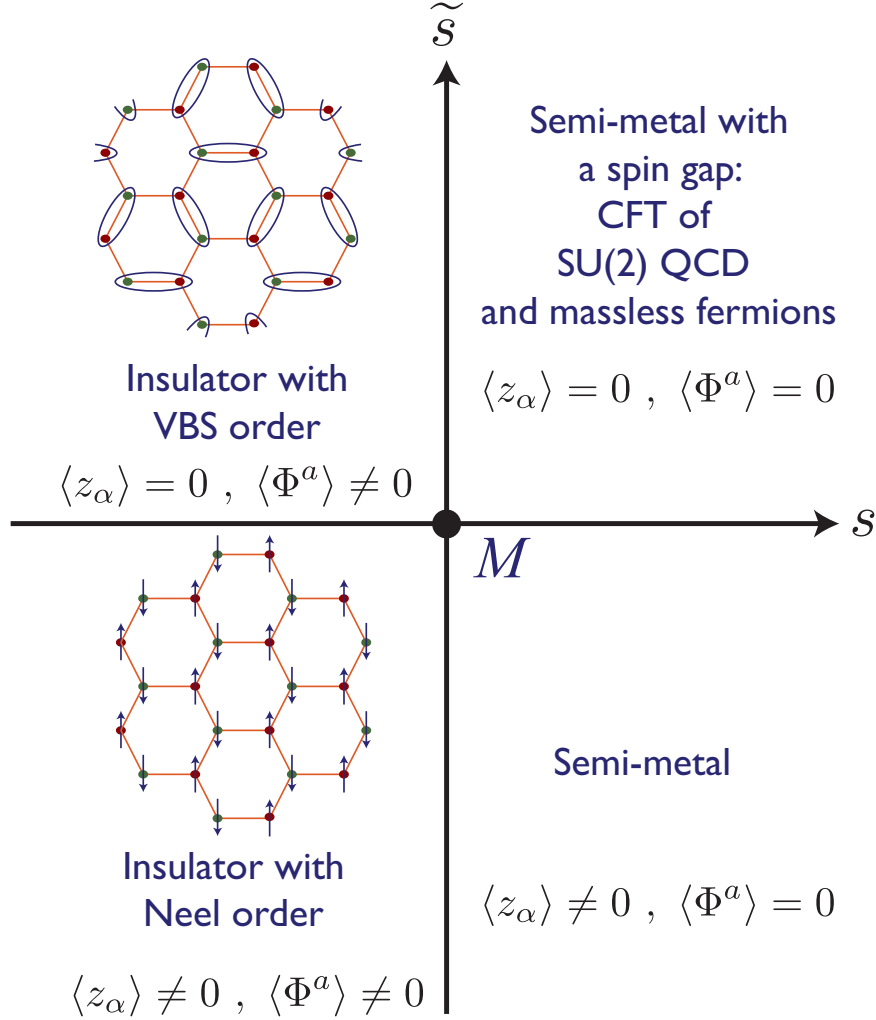


FIG. 11: Schematic phase diagram of the $SU(2)_g$ gauge theory \mathcal{L}_g in Eq. (5.4). The two phases in the bottom are described by the Gross-Neveu-Yukawa model in Eq. (2.27), while the two phases on the left are described by the $U(1)$ gauge theory $\mathcal{L}_z + \mathcal{L}_\Psi$ in Eqs. (4.3) and (4.7).

This QCD with a $SU(2)_g$ gauge group with massless 2-component Dirac fermions which carry $N_c = 2$ colors and $N_f = 2$ flavors. When N_f is large enough, it can be shown from a $1/N_f$ expansion that the confining tendencies of non-Abelian gauge fields are screened, and \mathcal{L}_{QCD} describes a non-trivial CFT, with anomalous dimensions for all observables which are not currents of global flavor or spacetime symmetries. It is an open question whether such a critical phase is allowed for $N_f = 2$, as we have assumed in Fig. 11. If not, then this phase will be unstable to confinement into one of the other phases of Fig. 11. If present, this deconfined phase would be a topologically ordered semi-metal with a spin gap; it is an ‘algebraic charge liquid’ (ACL) in the notation of Ref. 65. The gapless Ψ fermions carry electromagnetic charge, and so there is no gap to charged excitations and this phase is not an insulator. However, the Ψ fermions are spinless, and $SU(2)$ spin is only carried by the gapped bosonic excitations; hence the spin gap.

Fig 11 also shows an interesting multi-critical point M , where all 4 phases meet; if the massless QCD phase is confining, this would be the meeting point of 3 phases. Here the $SU(2)_g$ gauge bosons, the scalars Φ^a and R , and the fermions Ψ are all gapless and critical. Thus M realizes a non-trivial CFT which can be perturbed by the two relevant directions of the plane of Fig. 11. Indeed, it is not unreasonable to view this multicritical M theory as a non-supersymmetric analog of the M-theory of strings!

VI. THE METAL-INSULATOR TRANSITION ON THE TRIANGULAR LATTICE

This section will describe possible phases of the Hubbard model in Eq. (1.1) on the triangular lattice. We will now consider the case of generic density, so that unlike Sections II, IV, and V on the honeycomb lattice we will allow $\langle n_{i\uparrow} \rangle, \langle n_{i\downarrow} \rangle \neq 1/2$, although the half-filled density will also appear in our phase diagram. Unlike the honeycomb lattice, we will ignore the possibilities of magnetically ordered phases in which the global $SU(2)$ spin rotation symmetry is broken. The half-filled model on the triangular lattice likely does have antiferromagnetic order in the limit of large U , but we will not consider this complication here. Our purpose here is to describe the structure of possible phases without magnetic order.

The most significant difference from the honeycomb lattice is apparent in the limit of small U , when the electrons are nearly free. Then the triangular lattice ground state is a metal at all densities, unlike the semi-metal state found on the honeycomb lattice at half-filling. The semi-metal had a spectrum with a relativistic structure at low energies, a fact which we have exploited in our discussion so far. However the metal has zero energy excitations along a line in momentum space, the Fermi surface, and the fermionic excitations near the Fermi surface do not have a relativistic spectrum.

Landau's Fermi liquid (FL) theory provides a complete description of the universal properties of the metal. We will not review this theory here: the reader is referred to Chapter 18 of Ref. 19 for the author's perspective. A discussion in the context of the gauge-gravity duality appears in a recent paper⁵. For our purposes here, we need only two basic facts: (i) the fermionic excitations near the Fermi surface are essentially non-interacting electrons, and (ii) the area enclosed by the Fermi surface is equal to the electron density—this is Luttinger's theorem, which we state more explicitly below.

The FL metal can be described by ignoring the U interactions, and transforming Eq. (1.1) to momentum space. Unlike the honeycomb lattice, there is only one site per unit cell of the triangular lattice, and so the analog of Eq. (2.6) is now simply

$$H_0 = \sum_{\mathbf{k}} c_{\alpha}^{\dagger}(\mathbf{k}) \left[-\mu - 2t \left(\cos(\mathbf{k} \cdot \mathbf{e}_1) + \cos(\mathbf{k} \cdot \mathbf{e}_2) + \cos(\mathbf{k} \cdot \mathbf{e}_3) \right) \right] c_{\alpha}(\mathbf{k}), \quad (6.1)$$

where there are no Pauli matrices associated with sublattice index, the \mathbf{e}_i are as in Eq. (2.1),

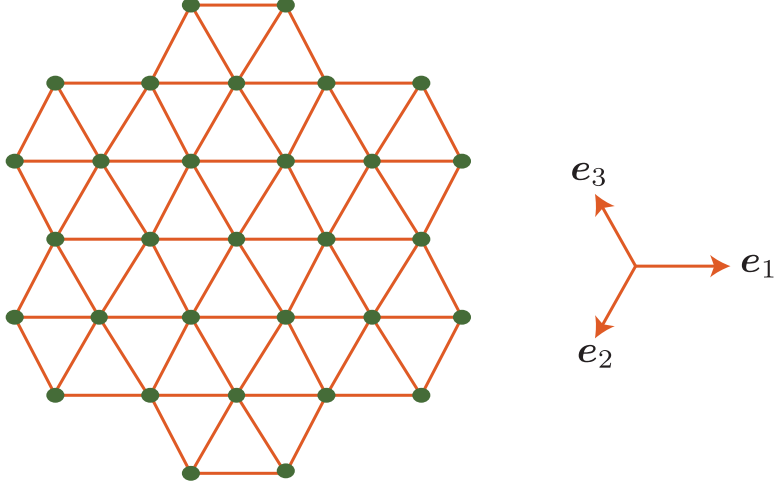


FIG. 12: The triangular lattice

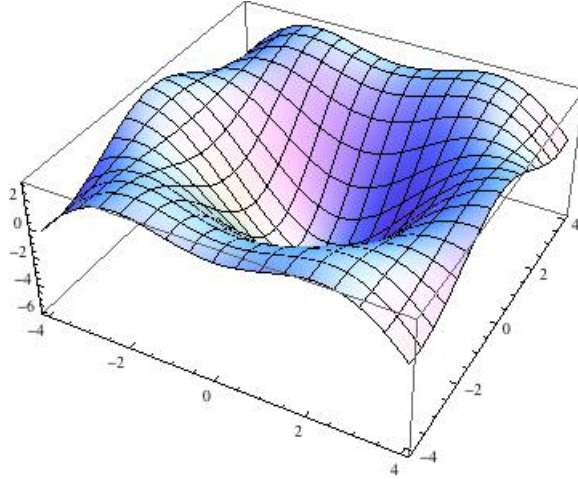


FIG. 13: The electronic dispersion in Eq. (6.1) for $\mu = 0$ and $t = 1$.

and are shown in Fig. 12. The reciprocal lattice now consists of the vectors $\sum_i n_i \mathbf{G}_i$, where Eq. (2.2) is replaced by

$$\mathbf{G}_1 = \frac{4\pi}{3}(\mathbf{e}_1 - \mathbf{e}_2) \quad , \quad \mathbf{G}_2 = \frac{4\pi}{3}(\mathbf{e}_2 - \mathbf{e}_3) \quad , \quad \mathbf{G}_3 = \frac{4\pi}{3}(\mathbf{e}_3 - \mathbf{e}_1), \quad (6.2)$$

while the first Brillouin zone is a hexagon with vertices given by Eq. (2.3), as shown in Fig. 14. The electronic dispersion in Eq. (6.1) is plotted in Fig. 13: it only has simple parabolic minima at $\mathbf{k} = 0$, and its periodic images at $\mathbf{k} = \mathbf{G}$, and there are no Dirac points. At any chemical potential, the negative energy states are occupied, leading to a Fermi surface bounding the set of occupied states, as shown in Fig. 14. Luttinger theorem states that the total area of the occupied states, the shaded region of the first Brillouin zone

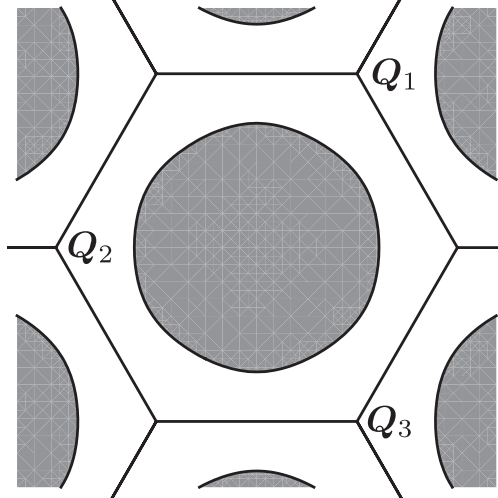


FIG. 14: The Fermi surface of Eq. (6.1) for $\mu = 1/2$ and $t = 1$; the occupied states are shaded. Also shown are the periodic images of the Fermi surface in their respective Brillouin zones.

in Fig. 14 occupies an area, \mathcal{A} , given by

$$\frac{\mathcal{A}}{2\pi^2} = \mathcal{N}, \quad (6.3)$$

where $\mathcal{N} = \sum_{\alpha} c_{\alpha}^{\dagger} c_{\alpha}$ is the total electron density. This relationship is obviously true for free electrons simply by counting occupied states, but it also remains true for interacting electrons, as reviewed recently in Ref. 5.

Now we turn up the strength of the interactions, U . For the honeycomb lattice, we presented in Sections II C and II D a treatment which allowed for the appearance of spontaneous magnetic moment on each site, leading to the onset of antiferromagnetic order at large U . We also found that the onset of antiferromagnetic order co-incident with appearance of the insulator *i.e.* the semi-metal to insulator transition. This co-incidence was related to the appearance of a gap in the spectrum even for an infinitesimal antiferromagnetic moment, as in Eq. (2.21). We can apply a similar treatment here to the triangular lattice. However, such an analysis finds that the onset of magnetic order does not co-incide with the metal-insulator transition. Instead, we find an intermediate metallic phase with magnetic order, in which the Fermi surface has been reconstructed into small ‘‘pockets’’. Such a reconstruction is observed in many correlated electron systems. However, we will not explore this route to the insulator here, and refer the reader to recent papers^{53,54}.

Instead, we will explore here a distinct route to the destruction of the Fermi liquid, one which reaches directly to an insulator which is a ‘spin liquid’^{55–57}. The spin liquid insulator is a phase in which the spin rotation symmetry is preserved, and there is a gap to all charged excitations. In these respects, the spin liquid is similar to the insulating state discussed in Section IV. However, in Section IV we found that such a insulator had an emergent $U(1)$ gauge field, A_{μ} , and the proliferation of monopole defects in A_{μ} led to a confining phase in

which lattice translational symmetry was broken by the appearance of VBS order. Here we will find that the triangular lattice spin liquid also has an emergent U(1) gauge field, but the presence of Fermi surfaces in the spinful excitations leads to the suppression of monopole events. Consequently, we have a deconfined phase with gapless gauge excitations, no lattice translational symmetry breaking, and the spin liquid character survives.

The key to the description of the metal insulator transition is exact rewriting of the Hubbard model in Eq. (1.1) as a compact U(1) lattice gauge theory. We proceed with a method which parallels that in Section IV, of transforming to a ‘rotating reference frame’. However, instead of using the frame of reference of local antiferromagnetic order, we use a quantum rotor to keep track of the charge on each lattice site. Each rotor has a periodic angular co-ordinate ϑ_i with period 2π ; hence the states of the rotors are $e^{in_{r_i}\vartheta_i}$ where n_{r_i} is a rotor angular momentum, whose eigenvalues take all positive and negative integer values. We will use the state with all $n_{r_i} = 0$ to represent the states with one electron each lattice site. The analog of the transformation to a rotating reference frame in Eq. (4.4) is now⁵⁸

$$c_\alpha = e^{-i\vartheta} f_\alpha \quad (6.4)$$

where we have dropped the implicit site index, and f_α are neutral fermions (‘spinons’) which keep track of the orientation of the electron. We can now identify the 4 states on each lattice site in Eq. (2.13) with corresponding states of the rotor and spinons:

$$\begin{aligned} |0\rangle &\Leftrightarrow e^{-i\vartheta}|0\rangle \\ c_\alpha^\dagger|0\rangle &\Leftrightarrow f_\alpha^\dagger|0\rangle \\ c_\uparrow^\dagger c_\downarrow^\dagger|0\rangle &\Leftrightarrow e^{i\vartheta} f_\uparrow^\dagger f_\downarrow^\dagger|0\rangle \end{aligned} \quad (6.5)$$

Note that these allowed states obey the constraint

$$f_\alpha^\dagger f_\alpha - n_r = 1. \quad (6.6)$$

Associated with this constraint is the U(1) gauge invariance which is the analog of Eqs. (4.2) and (4.5):

$$f_\alpha \rightarrow f_\alpha e^{i\zeta} \quad , \quad \vartheta \rightarrow \vartheta + \zeta. \quad (6.7)$$

Just as in Section IV, there will be an emergent gauge field A_μ in the effective theory of this model. The constraints in Eq. (6.6) will be the Gauss law of this theory.

First, let us rewrite the Hubbard model in terms of these new variables. Our degrees of freedom are the Fermi operators $f_{i\alpha}$ on each lattice site which obey the usual canonical fermion anti-commutation relations as in Eq. (1.3), and the rotor angle ϑ_i and angular momentum n_{r_i} which obey

$$[\vartheta_i, n_{r_j}] = i\delta_{ij}. \quad (6.8)$$

The Hubbard Hamiltonian in Eq. (1.1) is now exactly equivalent to

$$H[f, \vartheta] = - \sum_{i,j} t_{ij} f_{i\alpha}^\dagger f_{j\alpha} e^{i(\vartheta_i - \vartheta_j)} + \sum_i \left(-\mu(n_{ri} + 1) + \frac{U}{2} n_{ri}(n_{ri} + 1) \right), \quad (6.9)$$

provided our attention is restricted to the set of states which obey the constraint in Eq. (6.6) on every lattice site; note that the Hamiltonian in Eq. (6.9) commutes with constraints in (6.6), and so these can be consistently imposed. In Eq. (6.9) we have used the rotor angular momentum to measure the charge on each site, and so the dependence of the energy on μ and U can be expressed in terms of n_{ri} alone.

We can now implement the commutation relations, the Hamiltonian, and the constraint in a coherent state path integral

$$\begin{aligned} \mathcal{Z} = & \int \mathcal{D}f_{i\alpha}(\tau) \mathcal{D}f_{i\alpha}^\dagger(\tau) \mathcal{D}\vartheta_i(\tau) \mathcal{D}n_{ri}(\tau) \mathcal{D}\lambda_i(\tau) \exp \left(- \int d\tau H[f, \vartheta] \right. \\ & \left. - \int d\tau \sum_i \left[f_{i\alpha}^\dagger \frac{\partial f_{i\alpha}}{\partial \tau} - in_{ri} \frac{\partial \vartheta_i}{\partial \tau} + i\lambda_i (f_{i\alpha}^\dagger f_{i\alpha} - n_{ri} - 1) \right] \right), \end{aligned} \quad (6.10)$$

where $\vartheta_i(\tau)$ takes values on a circle with unit radius, ensuring quantization of eigenvalues of the angular momentum n_{ri} to integer values. The constraint in Eq. (6.6) is implemented using an auxiliary field $\lambda_i(\tau)$ which acts as a Lagrange multiplier.

A key observation now is that the partition function in Eq. (6.10) is invariant under a site, i , and τ -dependent U(1) gauge transformation $\zeta_i(\tau)$ where the fields transform as in Eq. (6.7), and λ transforms as

$$\lambda_i \rightarrow \lambda_i - \frac{\partial \zeta_i}{\partial \tau}. \quad (6.11)$$

In other words, λ transforms like the temporal component of a U(1) gauge field.

How do we obtain the spatial components of the gauge field? For this, we apply the Hubbard-Stratonovich transformation of Eq. (2.23) to the t_{ij} hopping term in Eq. (6.9). For this, we introduce another auxiliary complex field $Q_{ij}(\tau)$ which lives on the links of the triangular lattice and replace the hopping term by

$$\sum_{i,j} \left(\frac{|Q_{ij}(\tau)|^2}{t_{ij}} - Q_{ij}(\tau) f_{i\alpha}^\dagger f_{j\alpha} - Q_{ij}^*(\tau) e^{i(\vartheta_i - \vartheta_j)} \right) \quad (6.12)$$

We now see from Eq. (6.7), that Q_{ij} transforms under the gauge transformation in Eq. (6.7) as

$$Q_{ij} \rightarrow Q_{ij} e^{i(\zeta_i - \zeta_j)}. \quad (6.13)$$

In other words, $\arg(Q_{ij})$ is the needed spatial component of the compact U(1) gauge field.

So far, we have apparently only succeeded in making our analysis of the Hubbard model in

Eq. (1.1) more complicated. Instead of the functional integral of the single complex fermion $c_{i\alpha}$, we now have a functional integral over the complex fermions $f_{i\alpha}$, the rotor ϑ_i , and the auxilliary fields λ_i and Q_{ij} . How can this be helpful? The point, of course, is that the new variables help us access new phases and critical points which were inaccessible using the electron operators, and these phases have strong correlations which are far removed from those of weakly interacting electrons.

The utility of the new representation is predicated on the assumption that the fluctuations in the auxiliary fields Q_{ij} and λ_i are small along certain directions in parameter space. So let us proceed with this assumption, and describe the structure of the phases so obtained. We parameterize

$$Q_{ij} = \bar{Q}_{ij} e^{A_{ij}} \quad , \quad \lambda_i = -i\bar{\lambda} - A_{i\tau} \quad (6.14)$$

and ignore fluctuations in the complex numbers \bar{Q}_{ij} , and the real number $\bar{\lambda}$. With these definitions, it is clear from Eqs. (6.11) and (6.13) that A_{ij} and A_τ form the spatial and temporal components of a U(1) gauge field, and so must enter into all physical quantities in a gauge invariant manner. The values of \bar{Q}_{ij} and $\bar{\lambda}$ are determined by a suitable saddle-point analysis of the partition function, and ensure that the constraint (6.6) is obeyed. With these assumptions, the partition function separates into separate fermionic and rotor degrees of freedom interacting via their coupling to a common U(1) gauge field $(A_{i\tau}, A_{ij})$. In the continuum limit, the gauge fields become a conventional U(1) gauge field $A_\mu = (A_\tau, \mathbf{A})$. The partition function of the gauge theory is

$$\begin{aligned} \mathcal{Z} = & \int \mathcal{D}f_{i\alpha}(\tau) \mathcal{D}f_{i\alpha}^\dagger(\tau) \mathcal{D}\vartheta_i(\tau) \mathcal{D}n_{ri}(\tau) \mathcal{D}A_{i\tau}(\tau) \mathcal{D}A_{ij}(\tau) \\ & \exp \left(- \int d\tau \left[\mathcal{L}_f + \mathcal{L}_r + i \sum_i A_{i\tau} \right] \right) \\ \mathcal{L}_f = & \sum_i f_{i\alpha}^\dagger \left(\frac{\partial}{\partial \tau} + \bar{\lambda} - iA_{i\tau} \right) f_{i\alpha} - \sum_{ij} \bar{Q}_{ij} f_{i\alpha}^\dagger e^{iA_{ij}} f_{j\alpha} \\ \mathcal{L}_r = & -i \sum_i n_{ri} \left(\frac{\partial \vartheta_i}{\partial \tau} - A_{i\tau} \right) - \sum_{ij} \bar{Q}_{ij}^* e^{i(\vartheta_i - \vartheta_j - A_{ij})} \\ & + \sum_i \left(-\bar{\lambda} n_{ri} - \mu(n_{ri} + 1) + \frac{U}{2} n_{ri}(n_{ri} + 1) \right). \end{aligned} \quad (6.15)$$

Thus we have fermions $f_{i\alpha}$ moving in a band structure which is roughly the same as that of the electrons in Eq. (6.1), rotors which obey a boson Hubbard-like Hamiltonian, and both are minimally coupled to a compact U(1) gauge field.

We begin by neglecting the gauge fields, and computing the separate phase diagrams of \mathcal{L}_f and \mathcal{L}_r .

The fermions are free, and so occupy the negative energy states determined by the chemical potential $\bar{\lambda}$.

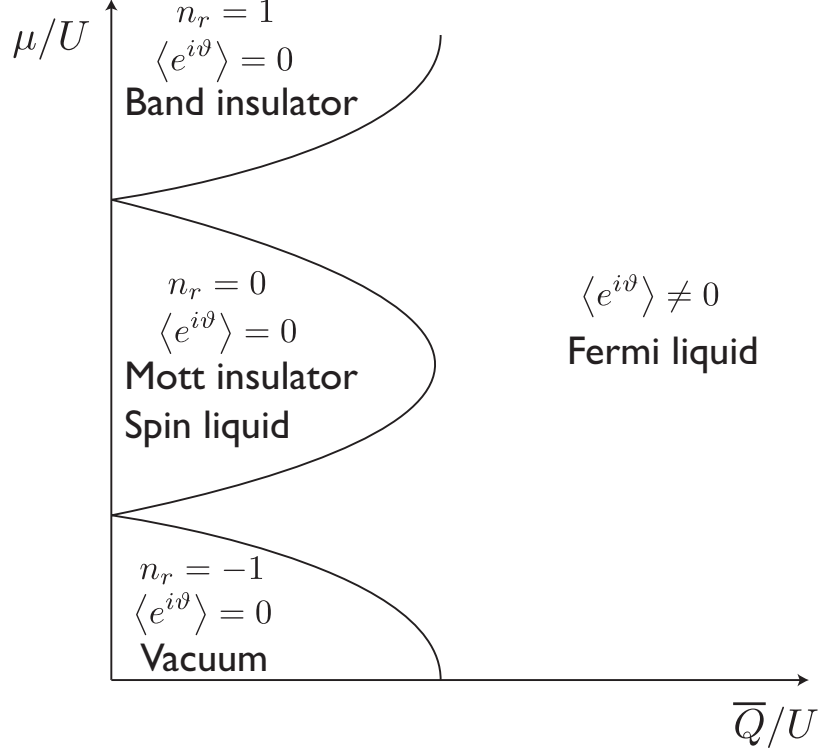


FIG. 15: Possible phase diagram of the electron Hubbard model in Eq. (1.1) on the triangular lattice. This phase diagram is obtained by a mean-field analysis of the theory \mathcal{L}_r in Eq. (6.15), similar to that for the boson Hubbard model in Chapter 9 of Ref. 19. Only the Mott insulating lobes with $n_r = -1, 0, 1$ are compatible with the constraint in Eq. (6.6); these Mott insulating lobes have fermion density $\langle f_\alpha^\dagger f_\alpha \rangle = n_r + 1$.

The phase diagram of \mathcal{L}_r is more interesting: it involves strong interactions between the rotors. It can be analyzed in a manner similar to that of the boson Hubbard model (see Chapter 9 of Ref. 19), leading to the familiar ‘‘Mott lobe’’ structure shown in Fig. 15.

At large values of \bar{Q}/U we have the analog of the superfluid states of the boson Hubbard model, in which there is a condensate of the rotor ladder operator $e^{i\vartheta}$. However, this operator is charged under the $U(1)$ gauge field, and so this phase does not break any global symmetries. Instead it is a Higgs phase, like the Néel phase in the model of Section IV. In the presence of the Higgs condensate, the operator relation in Eq. (6.4) implies that $c_\alpha \sim f_\alpha$, and so the f_α fermions carry the same quantum numbers as the physical electron. Consequently, the f_α Fermi surface is simply an electron Fermi surface. Furthermore, the Higgs condensate quenches the A_μ fluctuations, and so there are no singular interactions between the Fermi surface excitations. This identifies the present phase as the familiar Fermi liquid, as identified in Fig. 15.

Having reproduced a previously known phase of the Hubbard model in the $U(1)$ gauge theory, let us now examine the new phases within the ‘Mott lobes’ of Fig. 15. In these states, the rotor excitations are gapped, and the rotor angular momentum has integer expectation

values. The constraint in Eq. (6.6) implies that only $n_r = -1, 0, 1$ are acceptable values, and so only these values are shown. It is clear from the representation in Eq. (6.5) that any excitation involving change in electron number must involve a rotor excitation, and so the rotor gap implies a gap in excitations carrying non-zero electron number. This identifies the present phases as insulators. Thus the phase boundary out of the lobes in Fig. 15 is a metal-insulator transition.

Section VII B will present an explicit demonstration of the insulating and metallic properties of the phases in Fig. 15 by a computation of the transport properties of a broader class of models.

The three insulators in Fig. 15 have very different physical characteristics.

Using the constraint in Eq. (6.6) we see that the $n_r = -1$ insulator has no f_α fermions. Consequently this is just the trivial empty state of the Hubbard model, with no electrons.

Similarly, we see that the $n_r = 1$ insulator has 2 f_α fermions on each site. This is just the fully-filled state of the Hubbard model, with all electronic states occupied. It is a band insulator.

Finally, we turn to the most interesting insulator with $n_r = 0$. Now the electronic states are half-filled, with $\langle f_\alpha^\dagger f_\alpha \rangle = 1$. Thus there is an unpaired fermion on each site, and its spin is free to fluctuate. There is a non-trivial wavefunction in the spin sector, realizing an insulator which is a ‘spin liquid’. In our present mean field theory, the spin wavefunction is specified by Fermi surface state of the f_α fermions. Going beyond mean-field theory, we have to consider the fluctuations of the A_μ gauge field, and determine if they destabilize the spin liquid, as we did in earlier Section IV. Here the f_α fermions carry the A_μ gauge charge, and these fermions form a Fermi surface. This is a crucial difference from Section IV, where the ψ_\pm fermions were gapped. In Section IV we found that the monopoles proliferated, leading to confinement and VBS order. Here, the gapless fermionic excitations at the Fermi surface prevent the proliferation of monopoles: the low energy fermions suppress the tunneling event associated with global change in A_μ flux^{59,60}. Thus the emergent U(1) gauge field remains in a deconfined phase, and this spin liquid state is stable. These gapless gauge excitations have strong interactions with the f_α fermions, and this leads to strong critical damping of the fermions at the Fermi surface which is described by a strongly-coupled field theory^{61–63}. The effect of the gauge fluctuations is also often expressed in terms of an improved trial wavefunction for the spin liquid⁵⁵: we take the free fermion state of the f_α fermions, and apply a projection operator which removes all components which violate the constraint in Eq. (6.6). This yields the ‘Gutzwiller projected’ state

$$|\text{spin liquid}\rangle = \left(\prod_i \left[\frac{1 - (-1)^{\sum_\alpha f_{i\alpha}^\dagger f_{i\alpha}}}{2} \right] \right) \left(\prod_{\mathbf{k} < k_F} f_\uparrow^\dagger(\mathbf{k}) f_\downarrow^\dagger(\mathbf{k}) \right) |0\rangle, \quad (6.16)$$

where the product over \mathbf{k} is over all points inside the Fermi surface.

Finally, we turn to an interesting quantum phase transition in Fig. 15. This is the

transition between the spin liquid and the Fermi liquid at total electron density $\mathcal{N} = 1$, which occurs at the tip of the $n_r = 0$ Mott lobe. From the rotor sector, this looks like a Higgs transition, of the condensation of a complex scalar in the presence of a fluctuating U(1) gauge field. However, the fermionic sector is crucial in determining the nature of this transition. Indeed, in the absence of the Fermi surface, this transition would not even exist beyond mean field theory: this is because the U(1) gauge field is compact, and the scalar carries unit charge, and so the confining and Higgs phases of this gauge theory are smoothly connected. So we have to combine the Higgs theory of a complex scalar with the gapless Fermi surface excitations. Introducing a Bose field

$$b = e^{-i\vartheta}, \quad (6.17)$$

and coarse-graining to a continuum limit for the bosons, we find the field theory⁵⁷

$$\begin{aligned} \mathcal{L} = & |(\partial_\mu + iA_\mu)b|^2 + s|b|^2 + u|b|^4 + iA_\tau\mathcal{N} \\ & + f_\alpha^\dagger \left[\frac{\partial}{\partial\tau} + \epsilon_f - iA_\tau - \frac{1}{2m_f}(\nabla - i\mathbf{A})^2 \right] f_\alpha, \end{aligned} \quad (6.18)$$

where the energy ϵ_f is to be adjusted to yield total fermion density $\mathcal{N} = 1$. The transition is accessed by tuning s , and we move from a spin liquid for $s < s_c$, to a Fermi liquid for $s > s_c$. The critical properties of the theory in Eq. (6.18) have been studied^{57,64}, and an interesting result is obtained: the Fermi surface excitations damp the gauge bosons so that they become ineffective in coupling to the critical b fluctuations. Consequently, the gauge bosons can be ignored in the b fluctuations, and the transition is in the universality class of the 2+1 dimensional XY model.

VII. FRACTIONALIZED FERMION LIQUIDS

In Section VI we met the canonical description of a compressible metallic state, the Fermi liquid. This is the state adiabatically connected to the metallic state of non-interacting electrons. It has long-lived fermionic quasiparticle excitations along the Fermi surface, and the area enclosed by this Fermi surface obeys the Luttinger theorem.

Here we explore an extended model which allows for other compressible phases of strongly interacting electrons at generic densities which do not break any global symmetries, and which are not adiabatically connected to the limit of non-interacting electrons. We shall focus here on the compressible state^{2,3} known as the fractionalized Fermi liquid (FL*). In principle, the FL* state can appear in a variety of models of correlated electrons, including ones with a single band, and all the sites equivalent with $U_i = U$. Such single-band FL* states have been described in recent work⁶⁵⁻⁷¹. However, these single-band analyses are involved, and require intermediate steps which make them sub-optimal for a first description of the

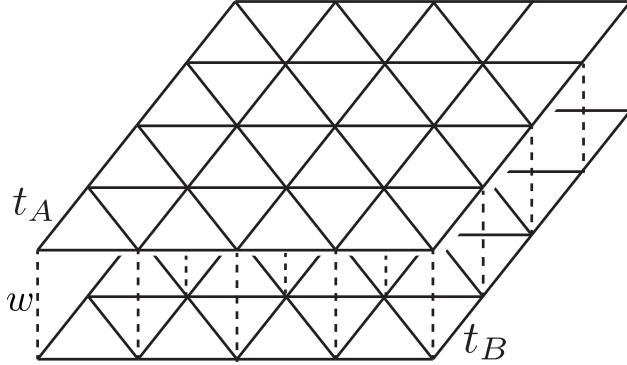


FIG. 16: The bilayer triangular lattice. The top layer (A) has nearest neighbor hopping t_A , the bottom layer (B) and nearest neighbor hopping t_B , and the inter-layer hopping is w . A closely related model is realized in the experiments of Ref. 6.

FL* state.

Instead, we will introduce the FL* state in a model with 2 types of inequivalent sites. As a simple example, consider the Hubbard model on a bilayer triangular lattice shown in Fig. 16. We label the two layers as A and B , and so there are 2 electron operators, $c_{Ai\alpha}$ and $c_{Bi\alpha}$. We write the Hamiltonian as

$$\begin{aligned}
 H &= H_A + H_B + H_{AB} \\
 H_A &= -t_A \sum_{\langle ij \rangle} c_{Ai\alpha}^\dagger c_{Aj\alpha} + \text{H.c.} + (\epsilon_A - \mu) \sum_i (n_{Ai\uparrow} + n_{Ai\downarrow}) \\
 &\quad + U_A \sum_i \left(n_{Ai\uparrow} - \frac{1}{2} \right) \left(n_{Ai\downarrow} - \frac{1}{2} \right) \\
 H_B &= -t_B \sum_{\langle ij \rangle} c_{Bi\alpha}^\dagger c_{Bj\alpha} + \text{H.c.} + (\epsilon_B - \mu) \sum_i (n_{Bi\uparrow} + n_{Bi\downarrow}) \\
 &\quad + U_B \sum_i \left(n_{Bi\uparrow} - \frac{1}{2} \right) \left(n_{Bi\downarrow} - \frac{1}{2} \right) \\
 H_{AB} &= -w \sum_i c_{Ai\alpha}^\dagger c_{Bi\alpha} + \text{H.c.}
 \end{aligned} \tag{7.1}$$

Here the sites i, j lie on a triangular lattice, and $\langle ij \rangle$ represents the sum over nearest-neighbor pairs. The Hubbard models on the two layers have distinct values of the hopping parameters, on-site repulsion, and on-site energies $\epsilon_{A,B}$. Finally, there is an on-site inter-layer tunneling, w . Experiments⁶ on bilayer films of ^3He adsorbed on graphite provide a remarkable realization of a closely related model.

First, let us discuss the FL state, where $U_{A,B}$ can be treated perturbatively. Diagonalizing

the one-electron Hamiltonian, we find two bands corresponding to the bonding and anti-bonding states between the two layers. Let \mathcal{N} be the total density of electrons for each bilayer site of the triangular lattice. So

$$\sum_{\alpha} \left(\left\langle c_{A\alpha}^{\dagger} c_{A\alpha} \right\rangle + \left\langle c_{B\alpha}^{\dagger} c_{B\alpha} \right\rangle \right) = \mathcal{N}. \quad (7.2)$$

This relation holds for every site i , and the site-index has been left implicit. Depending upon the value of \mathcal{N} and interlayer tunneling w , one or both of the bands will be occupied, leading to one or two Fermi surfaces. Let the areas enclosed by the Fermi surfaces be \mathcal{A}_1 and \mathcal{A}_2 ; if there is only one Fermi surface, $\mathcal{A}_2 = 0$. Luttinger's theorem fixes the areas of Fermi surfaces to a value which is independent of the nature of the electron-electron interactions. There is one Luttinger theorem for each global U(1) symmetry of the Hamiltonian which is not spontaneously broken in the ground state^{5,72,73}. Here, the total numbers of both up-spin and down-spin electrons are separately conserved, and so there are 2 Luttinger constraints. However, we will implicitly only consider states in which spin rotation invariance is preserved, and so there is only a single constraint. The constraint is the same as that for non-interacting electrons, which, as in Eq. (6.3), is

$$\frac{\mathcal{A}_1 + \mathcal{A}_2}{2\pi^2} = \mathcal{N}. \quad (7.3)$$

We will implicitly assume $\mathcal{N} > 1$ below.

We now wish to induce a quantum phase transition to a FL* state. This is most easily done in a model in which the bottom layer B has a density of one electron per site, while the top layer A remains dilute (as in the experiment in Ref. 6). For small hopping this is achieved for $U_A = U_B = U$ and

$$\epsilon_B < \epsilon_A < \epsilon_B + U. \quad (7.4)$$

Then the bottom layer B will acquire strong electronic correlations like those in Section VI, while the dilute gas on layer A can be treated perturbatively in the two-particle scattering amplitude. It is customary at this point to follow the analysis of Section II C, and project onto this restricted Hilbert space, while using a canonical transformation to derive an effective Hamiltonian. The restricted space has only spin degrees of freedom on B lattice sites, and as in Section II C, these spins have exchange interactions with each other. The canonical transformation also generates exchange interactions between electrons separate layers, and this is known as the Kondo exchange interaction. The resulting Hamiltonian is the Kondo-Heisenberg model. However, we will not take this step here, and continue to work with the Hubbard model in Eq. (7.1).

We will assume that layer B , with a density of one electron per site, realizes the spin liquid state discussed in Section VI; *i.e.* it is the $n_r = 0$ spin liquid in Fig. 15, with a spinon Fermi surface. We can obtain a description of this spin liquid by applying the analysis of

Section VI to layer. So we replace Eq. (6.4) by

$$c_{B\alpha} = e^{-i\vartheta} f_\alpha, \quad (7.5)$$

and perform the same transformations which led to Eq. (6.15). Then we take the same continuum limit as that used for Eq. (6.18), and obtain the following continuum Lagrangian \mathcal{L} which captures the low energy physics of the Hubbard model in Eq. (7.1). The degrees of freedom are the A layer electrons $c_{A\alpha}$, the B layer spinons f_α , and the bosonic rotors $b = e^{-i\vartheta}$ as in Eq. (6.17). The structure of the terms also follows from general considerations of gauge invariance and the preservation of global symmetries.

$$\begin{aligned} \mathcal{L} &= \mathcal{L}_f + \mathcal{L}_b + \mathcal{L}_c + iA_\tau \mathcal{N}_B \\ \mathcal{L}_f &= f_\alpha^\dagger \left[\frac{\partial}{\partial \tau} + \epsilon_f - iA_\tau - \frac{1}{2m_f} (\nabla - i\mathbf{A})^2 \right] f_\alpha \\ \mathcal{L}_b &= \left[(\partial_\mu - (\epsilon_r - \mu)\delta_{\mu\tau} - iA_\mu + iA_{\text{ext},\mu}) b^\dagger \right] \\ &\quad \times \left[(\partial_\mu + (\epsilon_r - \mu)\delta_{\mu\tau} + iA_\mu - iA_{\text{ext},\mu}) b \right] + s|b|^2 + u|b|^4 \\ \mathcal{L}_c &= c_{A\alpha}^\dagger \left[\frac{\partial}{\partial \tau} - \mu - iA_{\text{ext},\tau} - \frac{1}{2m_c} (\nabla - i\mathbf{A}_{\text{ext}})^2 \right] c_{A\alpha} \\ &\quad - w \left(c_{A\alpha}^\dagger b f_\alpha + b^\dagger f_\alpha^\dagger c_{A\alpha} \right) \end{aligned} \quad (7.6)$$

Here $A_\mu = (A_\tau, \mathbf{A})$ is an emergent U(1) gauge field; we have also introduced a non-fluctuating electromagnetic gauge field $A_{\text{ext},\mu}$ as a source term which couples to the current of the globally conserved electromagnetic charge; we have coarse-grained b to a complex scalar field with both amplitude and phase fluctuations; the symbol μ refers separately to the chemical potential and spacetime component, and the interpretation should be clear from the context; the final Yukawa term is allowed by the symmetries, and represents the inter-layer tunneling w ; the on-site energies ϵ_f and ϵ_r are related to ϵ_A and ϵ_B and have to be tuned so that the system obeys the density constraints to be discussed below.

To review, the continuum theory in Eq. (7.6) has a $U(1) \times U(1)_{\text{ext}}$ symmetry associated with the transformations

$$\begin{aligned} f_\alpha &\rightarrow f_\alpha e^{i\zeta} \quad , \quad b \rightarrow b^{-i\zeta} \quad , \quad c_{A\alpha} \rightarrow c_{A\alpha} \\ f_\alpha &\rightarrow f_\alpha \quad , \quad b \rightarrow b^{i\tilde{\zeta}} \quad , \quad c_{A\alpha} \rightarrow c_{A\alpha} e^{i\tilde{\zeta}} \end{aligned} \quad (7.7)$$

The first U(1) symmetry is gauged by the dynamical emergent U(1) gauge field A_μ , and is the same as that in Eq. (6.7). The second U(1) symmetry remains global; the fixed external electromagnetic field $A_{\text{ext},\mu}$ couples a source term which gauges this global symmetry.

In general, there will be 2 Luttinger constraints associated with these two U(1) symmetries^{5,72,73} (as before, we are ignoring spin rotation symmetries here, which is as-

sumed to be always fully preserved). The first transformation in Eq. (7.7) leads to a Luttinger constraint on the associated conserved charge density (which is the continuum analog of Eq. (6.6))

$$\sum_{\alpha} \langle f_{\alpha}^{\dagger} f_{\alpha} \rangle - \langle \mathcal{Q}_b \rangle = \frac{\mathcal{A}_1}{2\pi^2} = \mathcal{N}_B. \quad (7.8)$$

Here \mathcal{N}_B is the density of electrons on layer B in the projected Hilbert space: our present lattice derivation was for $\mathcal{N}_B = 1$, but the continuum theory in Eq. (7.6) is sensible for any value of \mathcal{N}_B . The operator \mathcal{Q}_b is the rotor angular momentum, given by

$$\mathcal{Q}_b = -\frac{\partial \mathcal{L}_b}{\partial \mu}. \quad (7.9)$$

Thus there must be a Fermi surface enclosing area \mathcal{A}_1 , which counts the density of f fermions minus the bosonic rotor density.

Similarly, the second transformation of Eq. (6.6) leads to the constraint

$$\sum_{\alpha} \langle c_{A\alpha}^{\dagger} c_{A\alpha} \rangle + \langle \mathcal{Q}_b \rangle = \frac{\mathcal{A}_2}{2\pi^2} = \mathcal{N} - \mathcal{N}_B. \quad (7.10)$$

Again, there is a Fermi surface enclosing area \mathcal{A}_2 which counts the density of c_A fermions minus the bosonic rotor density. Thus our analysis so far appears to imply that there must be at least 2 Fermi surfaces, and their areas are constrained by the two independent relations in Eqs. (7.8) and (7.10).

This last conclusion seems rather surprising from our discussion above of the FL phase. There we found only a single constraint in Eq. (7.3) for the total areas of one or more Fermi surfaces. The only possible conclusion is that the FL phase is *not* one in which the $U(1) \times U(1)_{\text{ext}}$ symmetry of the Lagrangian \mathcal{L} in Eq. (7.6) remains unbroken. Rather the FL phase is realized as a Higgs phase in which the $U(1) \times U(1)_{\text{ext}}$ symmetry in Eq. (7.7) is broken down to a diagonal $U(1)$. Just as in Section VI, this is the Higgs phase in which the boson b condenses

$$\langle b \rangle \neq 0 \text{ in the FL phase.} \quad (7.11)$$

Once the symmetry is broken in this manner, the corresponding Luttinger constraint no longer applies^{5,72,73}. Only the *sum* of the constraints in Eqs. (7.8) and (7.10) applies, and this leads immediately to the defining relation in Eq. (7.3) of the FL phase. The condensation of b also quenches the emergent $U(1)$ gauge field, so there are no gapless gauge excitations in the FL state, again as in Section VI.

We now see that state of the theory \mathcal{L} in which the Luttinger constraints in Eqs. (7.8) and (7.10) apply separately is a new phase: this is the advertised FL* phase, in which the boson b is uncondensed^{2,3}

$$\langle b \rangle = 0 \text{ in the FL* phase.} \quad (7.12)$$

The full $U(1)\times U(1)_{\text{ext}}$ symmetry is preserved, and the gauge boson A_μ becomes an emergent gapless photon. The arguments for the stability of the FL* phase towards gauge fluctuations mirror those of Section VI for the stability of the spinon Fermi surface in the spin liquid.

The criteria in Eqs. (7.11) and (7.12) show that the transition between the FL and FL* states is tuned by varying the coupling s in \mathcal{L}_b from negative to positive values. The transition between these phases occurs at a quantum critical point where the scalar b is also critical.

A. Connections to holographic metals

We now connect the above generic theory of the compressible FL and FL* phases of the Hubbard model to recent studies of compressible metallic phases via the AdS/CFT correspondence. The discussion below refers to recent work from the gravity perspective; an analysis starting from the canonical supersymmetric gauge theories of gauge-gravity duality may be found in Ref. 5.

A connection was made in Ref. 4 between a mean-field solution of models like the Hubbard model in Eq. (7.1) and a particular AdS realization of a holographic metal. Specifically, the bilayer Hubbard model has been solved in a limit with infinite-range hopping matrix elements between the sites (in contrast to the nearest-neighbor hopping shown in Eq. (7.1)). A detailed correspondence was found between the low energy properties of the FL* phase of such a model and the holographic theory^{24,74,75} in which the low energy limit factorized to a $\text{AdS}_2\times\mathbb{R}^d$ geometry (d is the dimensionality of space). This work has been recently reviewed in the companion article¹.

However, the mean-field solution of Eq. (7.1) and the $\text{AdS}_2\times\mathbb{R}^d$ geometry share a number of artifacts: they have a non-zero ground state entropy, and the spin correlations of layer B scale with dynamic exponent $z = \infty$. These artifacts are not expected to be properties of the field theory \mathcal{L} in Eq. (7.6), applicable for models with short-range interactions.

It is clearly of interest to move beyond the $\text{AdS}_2\times\mathbb{R}^d$ factorization in the holographic theory, and derive a holographic model which has a closer correspondence with the phases of the field theory in Eq. (7.6). A number of recent theories^{75–84} have examined the feedback of the finite density matter on the metric of the AdS space, and found that the AdS_2 horizon disappears at $T = 0$, and is replaced by a metric with a finite value of z . Many physical properties of such holographic metals are similar to those of the field theory in Eq. (7.6), but a detailed correspondence awaits future work.

It is useful to consider these recent works in the context of a holographic RG^{74,75,85–88}. In these works, the UV degrees of freedom are coupled to external sources, which in our case is $A_{\text{ext},\mu}$. Then an effective action is derived which couples the external sources to the IR degrees of freedom. Two distinct fixed-point theories have been considered in the literature: those of Nickel and Son⁸⁵, and of Faulkner *et al.*⁷⁴ and Faulkner and Polchinski⁷⁵. We argue

here that these fixed points capture the physics of the FL and FL* phases respectively.

Let us consider, first, the theory of Nickel and Son⁸⁵. They argued that the low energy theory had an emergent U(1) gauge field, so that the theory had a $U(1)_{\text{global}} \times U(1)_{\text{gauge}}$ symmetry. This is strikingly similar to the $U(1) \times U(1)_{\text{ext}}$ symmetry of Eq. (7.6). Indeed, we can more closely map the low energy theory of the FL phase of Eq. (7.6) to the model proposed by Nickel and Son. In the FL phase, we condense the b boson, and focus on the fluctuations of its phase $b = e^{-i\vartheta}$. Then the effective theory of the FL phase of Eq. (7.6) is

$$\mathcal{L}_{FL} = K_1 (\partial_\tau \vartheta - A_\tau + A_{\text{ext},\tau})^2 + K_2 (\nabla \vartheta - \mathbf{A} + \mathbf{A}_{\text{ext}})^2 + \Pi_f(A_\mu) + \mathcal{L}_c, \quad (7.13)$$

where Π_f is the effective action obtain after integrating out the f spinons. The structure of Eq. (7.13) is essentially identical to Eqs. (6) and (52) of Nickel and Son⁸⁵.

Consider, next, the corresponding low-energy theory of FL* phase. Now the b field is not condensed, and has an energy gap, Δ . So we can safely integrate it out from Eq. (7.6), and obtain an effective theory for the electrons, the spinons, and the gauge fields:

$$\begin{aligned} \mathcal{L}_{FL*} = & \mathcal{L}_f + J_1 \left(c_{A\alpha}^\dagger \sigma_{\alpha\beta}^a c_{A\beta} \right) (f_\gamma^\dagger \sigma_{\gamma\delta}^a f_\delta) + J_2 \left(c_{A\alpha}^\dagger c_{A\alpha} \right) (f_\gamma^\dagger f_\gamma) + \mathcal{L}_c \\ & + K_3 [\nabla(A_\tau - A_{\text{ext},\tau}) - \partial_\tau(\mathbf{A} - \mathbf{A}_{\text{ext}})]^2 + K_4 [\nabla \times (\mathbf{A} - \mathbf{A}_{\text{ext}})]^2, \end{aligned} \quad (7.14)$$

where $J_1 \sim J_2 \sim w^2/\Delta$. The coupling J_1 is the Kondo exchange between the electrons in layer A and the spins on layer B , while J_2 couples density fluctuations of the two layers. A key property of the FL* phase is that the couplings $J_{1,2}$ can be treated perturbatively: there is no flow to strong coupling in the Kondo exchange, and the layer B spins are not screened by the conduction electrons. Let us now rewrite the matter component of Eq. (7.14) as

$$\mathcal{L}_{FL*} = \mathcal{L}_f - \frac{1}{2} \left[F_\alpha^\dagger c_{A\alpha} + c_{A\alpha}^\dagger F_\alpha \right] + \mathcal{L}_c + \dots \quad (7.15)$$

where F_α is a IR fermion defined by⁴

$$F_\alpha \equiv -J_1 (\sigma_{\alpha\beta}^a f_\gamma^\dagger \sigma_{\gamma\delta}^a f_\delta) c_{A\beta} - J_2 (f_\gamma^\dagger f_\gamma) c_{A\alpha}. \quad (7.16)$$

Notice that both fermions in the displayed term in Eq. (7.15) are invariant under the emergent U(1); this term is a coupling between the microscopic fermion $c_{A\alpha}$ and a composite gauge-invariant fermion operator F_α representing the IR degrees of freedom. We can view F_α in Eq. (7.16) as the most general fermion operator which involves the IR fermions f_α , which is invariant under the gauge transformation associated with A_μ , and which also carries the global electron number charge associated with $A_{\text{ext},\mu}$. Then structure of Eq. (7.15) is precisely that of the semi-holographic theory of Faulkner *et al.*⁷⁴ and Faulkner and Polchinski⁷⁵, and their IR fermion F_α is chosen by essentially identical criteria.

It would clearly be of interest to also find another fixed point of the holographic theory

corresponding to the quantum-critical points between the FL and FL* phases.

B. Transport theory

We conclude our discussion of FL and FL* phases by presenting a general formulation of their transport properties. The arguments below are in the spirit of those of Ioffe and Larkin⁸⁹.

We begin with a theory like \mathcal{L} in Eq. (7.6), and integrate out the matter fields to obtain a Coleman-Weinberg effective action for the $U(1) \times U(1)$ gauge fields A_μ and $A_{\text{ext},\mu}$. In general, the form of this effective action is constrained only spatial isotropy and gauge invariance. Using the projectors defined in Eq. (3.13), we can write the quadratic portion of the effective action in the following form (we work here in Euclidean time, and ω_n is a Matsubara frequency)

$$\begin{aligned} \mathcal{S} = \frac{1}{2}T \sum_{\omega_n} \int \frac{d^2k}{4\pi^2} & \left[A_\mu \left(P_{\mu\nu}^L K_f^L(\omega_n, k) + P_{\mu\nu}^T K_f^T(\omega_n, k) \right) A_\nu \right. \\ & + (A_\mu - A_{\text{ext},\mu}) \left(P_{\mu\nu}^L K_b^L(\omega_n, k) + P_{\mu\nu}^T K_b^T(\omega_n, k) \right) (A_\mu - A_{\text{ext},\mu}) \\ & \left. + A_{\text{ext},\mu} \left(P_{\mu\nu}^L K_c^L(\omega_n, k) + P_{\mu\nu}^T K_c^T(\omega_n, k) \right) A_{\text{ext},\mu} \right] \end{aligned} \quad (7.17)$$

Here $K_f^{L,T}$ are given by the correlator of the current of the f fermions, $K_c^{L,T}$ by the correlator of the current of the c_A fermions, and $K_b^{L,T}$ by the current of the bosonic b rotors. Note that, unlike Eq. (3.12), we have not pulled out a factor of $\sqrt{k^2 + \omega_n^2}$ in the definition of the $K^{L,T}$. In general, determining these functions requires a complex transport analysis of the theory in Eq. (7.6). However, in the FL and FL* phases, the simpler low energy effective theories in Eqs. (7.13) and (7.14) lead to simple forms for the bosonic correlators $K_b^{L,T}$.

In the FL phase, integrating out the phase ϑ in Eq. (7.13) we obtain

$$K_b^L(\omega_n, k) = \frac{K_1 K_2 (k^2 + \omega_n^2)}{K_2 k^2 + K_1 \omega_n^2}, \quad K_b^T(\omega_n, k) = K_2. \quad (7.18)$$

Thus $K_b^{L,T}$ are constants in the limits of small momenta or frequency. Indeed, had we chosen the velocity of ‘light’ judiciously in the definition of $P_{\mu\nu}^L$ in Eq. (3.13), we would have had $K_b^L(\omega_n) = K_1$.

In contrast, in the FL* phase, we can directly match the low energy theory in Eq. (7.14) to Eq. (7.17) and obtain

$$K_b^L(\omega_n, k) = K_3 (k^2 + \omega_n^2), \quad K_b^T(\omega_n, k) = K_3 \omega_n^2 + K_4 k^2. \quad (7.19)$$

Now the $K_b^{L,T}$ vanish in the limit of small momentum and frequency.

We need to use the respective low energy theories of the FL and FL* phases in Eqs. (7.13) and (7.14) to determine $K_c^{L,T}$ and $K_f^{L,T}$, and then combine them with the above results for $K_b^{L,T}$ to obtain the physical conductivity. As in Nickel and Son⁸⁵, and in Ioffe and Larkin⁸⁹, this is obtained by implementing the equation of motion of the emergent gauge field A_μ in Eq. (7.17). This equation of motion is equivalent to the constraint that the current of the b bosons must equal the current of the f fermions, which is a consequence of the lattice constraint in Eq. (6.6). Evaluating the equation of motion $\delta\mathcal{S}/\delta A_\mu = 0$ from Eq. (7.17), and substituting the resulting value of A_μ back (after suitable gauge fixing), we obtain an effective action for the probe field $A_{\text{ext},\mu}$ alone

$$\mathcal{S}_{\text{ext}} = \frac{1}{2}T \sum_{\omega_n} \int \frac{d^2k}{4\pi^2} A_{\text{ext},\mu} \left(P_{\mu\nu}^L K_{\text{ext}}^L(\omega_n, k) + P_{\mu\nu}^T K_{\text{ext}}^T(\omega_n, k) \right) A_{\text{ext},\mu} \quad (7.20)$$

with

$$\begin{aligned} K_{\text{ext}}^L(\omega_n, k) &= K_c^L(\omega_n, k) + \frac{K_f^L(\omega_n, k)K_b^L(\omega_n, k)}{K_f^L(\omega_n, k) + K_b^L(\omega_n, k)} \\ K_{\text{ext}}^T(\omega_n, k) &= K_c^T(\omega_n, k) + \frac{K_f^T(\omega_n, k)K_b^T(\omega_n, k)}{K_f^T(\omega_n, k) + K_b^T(\omega_n, k)} \end{aligned} \quad (7.21)$$

After analytic continuation to Minkowski space, these results lead to the physical conductivity via the Kubo formula in Eq. (2.33)

$$\sigma(\omega) = \frac{i}{\omega} K_{\text{ext}}^L(\omega, 0). \quad (7.22)$$

The distinction from Eq. (3.15) is a consequence of omitting in Eq. (7.17) the prefactor $\sqrt{\omega_n^2 + k^2}$ present in Eq. (3.12).

These expressions can be used along with specific computations of the dynamics of the f and c fermions: the latter can be carried out either using a Boltzmann theory of the continuum model in Eq. (7.6), or via a theory on AdS. The analysis by Nickel and Son⁸⁵ for their holographic theory is equivalent to the application of Eq. (7.21). Let us verify that the present method yields the expected FL behavior in the Higgs phase where Eq. (7.18) implies that $K_b^L(\omega, 0) = K_2$. We assume that c and f Fermi surfaces have metallic conduction with $K_c^L(\omega, 0) = -i\omega\sigma_c$ and $K_f^L(\omega, 0) = -i\omega\sigma_f$, with $\sigma_{c,f}$ the respective conductivities. Inserting these expressions in Eq. (7.22), we obtain the expected FL behavior with $\sigma = \sigma_c + \sigma_f$ in the limit $\omega \rightarrow 0$. Thus there is no superfluidity associated with the condensation of b , and the gauge fluctuations lead eventually to metallic behavior. Similarly, it is easy to show that if b and c excitations are gapped, we have insulating transport, even though the f spinons have a gapless Fermi surface.

Further theoretical work exploring the connection between the AdS and Boltzmann ap-

proaches to transport is clearly of interest.

Acknowledgements

I am very grateful to the participants of TASI 2010 in Boulder, and of the ICTS Chandrasekhar Lecture Series and Discussion Meeting on “Strongly Correlated Systems and AdS/CFT” in Bangalore, Dec 2010. Many of the ideas presented here were developed and sharpened during discussions at these meetings. This research was supported by the National Science Foundation under grant DMR-0757145 and by a MURI grant from AFOSR.

-
- ¹ S. Sachdev, “Strange metals and the AdS/CFT correspondence,” *J. Stat. Mech.* **1011**, P11022 (2011) [arXiv:1010.0682 [cond-mat.str-el]].
 - ² T. Senthil, S. Sachdev, and M. Vojta, “Fractionalized Fermi liquids,” *Phys. Rev. Lett.* **90**, 216403 (2003) [arXiv:cond-mat/0209144].
 - ³ T. Senthil, M. Vojta, and S. Sachdev, “Weak magnetism and non-Fermi liquids near heavy-fermion critical points,” *Phys. Rev. B* **69**, 035111 (2004) [arXiv:cond-mat/0305193].
 - ⁴ S. Sachdev, “Holographic metals and the fractionalized Fermi liquid,” *Phys. Rev. Lett.* **105**, 151602 (2010) [arXiv:1006.3794 [hep-th]].
 - ⁵ L. Huijse and S. Sachdev, “Fermi surfaces and gauge-gravity duality,” arXiv:1104.5022 [hep-th].
 - ⁶ M. Neumann, J. Nyéki, B. Cowan, and J. Saunders, “Bilayer ^3He : A Simple Two-Dimensional Heavy-Fermion System with Quantum Criticality,” *Science* **317**, 1356 (2007).
 - ⁷ C. Cohen-Tannoudji, J. Dupont-Roc, and G. Grynberg, *Atom-Photon Interactions: Basic Processes and Applications*, Complement B₁, Wiley-VCH (1998).
 - ⁸ Z. Y. Meng, T. C. Lang, S. Wessel, F. F. Assaad, and A. Muramatsu, “Quantum spin-liquid emerging in two-dimensional correlated Dirac fermions,” *Nature* **464**, 847 (2010) [arXiv:1003.5809 [cond-mat.str-el]].
 - ⁹ M. Hermele, “SU(2) gauge theory of the Hubbard model and application to the honeycomb lattice,” *Phys. Rev. B* **76**, 035125 (2007) [arXiv:cond-mat/0701134].
 - ¹⁰ F. Wang, “Schwinger Boson Mean Field Theories of Spin Liquid States on Honeycomb Lattice: Projective Symmetry Group Analysis and Critical Field Theory,” *Phys. Rev. B* **82**, 024419 (2010) [arXiv:1004.2693 [cond-mat.str-el]].
 - ¹¹ Y. -M. Lu and Y. Ran, “Spin liquids on a honeycomb lattice: Projective Symmetry Group study of Schwinger fermion mean-field theory,” arXiv:1005.4229 [cond-mat.str-el].
 - ¹² Y. -M. Lu and Y. Ran, “ Z_2 spin liquid and chiral antiferromagnetic phase in Hubbard model on the honeycomb lattice: Duality between Schwinger-fermion and Schwinger-boson representations,” arXiv:1007.3266 [cond-mat.str-el].

- ¹³ C. Xu and S. Sachdev, “Majorana liquids: the complete fractionalization of the electron,” *Phys. Rev. Lett.* **105**, 057201 (2010) [arXiv:1004.5431 [cond-mat.str-el]].
- ¹⁴ C. Xu, “Quantum Spin Hall, triplet Superconductor, and topological liquid on the honeycomb lattice,” arXiv:1010.0455 [cond-mat.str-el].
- ¹⁵ I. F. Herbut, “Interactions and phase transitions on graphene’s honeycomb lattice,” *Phys. Rev. Lett.* **97**, 146401 (2006) [arXiv:cond-mat/0606195].
- ¹⁶ I. F. Herbut, V. Juricic, and B. Roy, “Theory of interacting electrons on the honeycomb lattice,” *Phys. Rev. B* **79**, 085116 (2009) [arXiv:0811.0610 [cond-mat.str-el]].
- ¹⁷ I. F. Herbut, V. Juricic, and O. Vafek, “Relativistic Mott criticality in graphene,” *Phys. Rev. B* **80**, 075432 (2009) [arXiv:0904.1019 [cond-mat.str-el]].
- ¹⁸ S. Sachdev, “Quantum phase transitions of correlated electrons in two dimensions,” *Physica A* **313**, 252 (2002) [arXiv:cond-mat/0109419].
- ¹⁹ S. Sachdev, *Quantum Phase Transitions*, 2nd ed., Cambridge (2011).
- ²⁰ V. M. Pereira, F. Guinea, J. M. B. Lopes dos Santos, N. M. R. Peres, and A. H. Castro Neto, “Disorder Induced Localized States in Graphene,” *Phys. Rev. Lett.* **96**, 036801 (2006) [arXiv:cond-mat/0508530].
- ²¹ S. Sachdev, C. Buragohain, and M. Vojta, “Quantum impurity in a nearly-critical two dimensional antiferromagnet,” *Science* **286**, 2479 (1999) [arXiv:cond-mat/0004156].
- ²² M. Vojta, C. Buragohain, and S. Sachdev, “Quantum impurity dynamics in two-dimensional antiferromagnets and superconductors,” *Phys. Rev. B* **61**, 15152 (2000) [arXiv:cond-mat/9912020].
- ²³ S. Sachdev, “Static hole in a critical antiferromagnet: field-theoretic renormalization group, S. Sachdev, *Physica C* **357**, 78 (2001) [arXiv:cond-mat/0011233].
- ²⁴ S. Kachru, A. Karch, and S. Yaida, “Holographic Lattices, Dimers, and Glasses,” *Phys. Rev. D* **81**, 026007 (2010) [arXiv:0909.2639 [hep-th]].
- ²⁵ S. Sachdev, “Non-zero temperature transport near fractional quantum Hall critical points,” *Phys. Rev. B* **57**, 7157 (1998) [arXiv:cond-mat/9709243].
- ²⁶ K. Damle and S. Sachdev, “Non-zero temperature transport near quantum critical points,” *Phys. Rev. B* **56**, 8714 (1997) [arXiv:cond-mat/9705206].
- ²⁷ L. Fritz, J. Schmalian, M. Müller, and S. Sachdev, “Quantum critical transport in clean graphene,” *Phys. Rev. B* **78**, 085416 (2008) [arXiv:0802.4289 [cond-mat.str-el]].
- ²⁸ M. Müller, L. Fritz, and S. Sachdev, “Quantum critical relativistic magnetotransport in graphene,” *Phys. Rev. B* **78**, 115406 (2008) [arXiv:0805.1413 [cond-mat.str-el]].
- ²⁹ I. F. Herbut, V. Juricic, and O. Vafek, “Coulomb interaction, ripples, and the minimal conductivity of graphene,” *Phys. Rev. Lett.* **100** 046403 (2008) [arXiv:0707.4171 [cond-mat.mes-hall]].
- ³⁰ V. Juricic, O. Vafek, I. F. Herbut, “Conductivity of interacting massless Dirac particles in graphene: Collisionless regime,” arXiv:1009.3269 [cond-mat.mes-hall].
- ³¹ L. Fritz, “Quantum-Critical transport at a semimetal-to-insulator transition on the honeycomb lattice,” arXiv:1012.0263 [cond-mat.str-el].

- ³² C. P. Herzog, P. Kovtun, S. Sachdev and D. T. Son, “Quantum critical transport, duality, and M-theory,” *Phys. Rev. D* **75**, 085020 (2007) [arXiv:hep-th/0701036].
- ³³ R. C. Myers, S. Sachdev, and A. Singh, “Holographic Quantum Critical Transport without Self-Duality,” *Phys. Rev. D* **83**, 066017 (2011) [arXiv:1010.0443 [hep-th]].
- ³⁴ S. Sachdev and X. Yin, “Quantum phase transitions beyond the Landau-Ginzburg paradigm and supersymmetry,” *Annals Phys.* **325**, 2 (2010) [arXiv:0808.0191 [cond-mat.str-el]].
- ³⁵ C. Dasgupta and B. I. Halperin, “Phase Transition in a Lattice Model of Superconductivity,” *Phys. Rev. Lett.* **47**, 1556 (1981).
- ³⁶ P. Kovtun, D. T. Son and A. O. Starinets, “Viscosity in strongly interacting quantum field theories from black hole physics,” *Phys. Rev. Lett.* **94**, 111601 (2005) [arXiv:hep-th/0405231].
- ³⁷ M. Müller, J. Schmalian, and L. Fritz, “Graphene - a nearly perfect fluid,” *Phys. Rev. Lett.* **103**, 025301 (2009) [arXiv:0903.4178 [cond-mat.str-el]].
- ³⁸ B. I. Shraiman and E. D. Siggia, “Mobile Vacancies in a Quantum Heisenberg Antiferromagnet,” *Phys. Rev. Lett.* **61**, 467 (1988).
- ³⁹ H. J. Schulz, “Effective action for strongly correlated fermions from functional integrals,” *Phys. Rev. Lett.* **65**, 2462 (1990).
- ⁴⁰ S. Sachdev, M. A. Metlitski, Y. Qi, and Cenke Xu, “Fluctuating spin density waves in metals,” *Phys. Rev. B* **80**, 155129 (2009) [arXiv:0907.3732 [cond-mat.str-el]].
- ⁴¹ A. D’Adda, P. Di Vecchia, and M. Lüscher, “A $1/n$ Expandable Series of Nonlinear Sigma Models with Instantons,” *Nucl. Phys.* **B 146**, 63 (1978).
- ⁴² E. Witten, “Instantons, the Quark Model, and the $1/n$ Expansion,” *Nucl Phys.* **B149**, 285 (1979).
- ⁴³ N. Read and S. Sachdev, “Spin-Peierls, valence bond solid, and Neel ground states of low dimensional quantum antiferromagnets,” *Phys. Rev. B* **42**, 4568 (1990).
- ⁴⁴ O. I. Motrunich and A. Vishwanath, “Emergent photons and new transitions in the O(3) sigma model with hedgehog suppression,” *Phys. Rev. B* **70**, 075104 (2004) [arXiv:cond-mat/0311222].
- ⁴⁵ T. Senthil, A. Vishwanath, L. Balents, S. Sachdev, and M. P. A. Fisher, “Deconfined quantum critical points,” *Science* **303**, 1490 (2004) [arXiv:cond-mat/0311326].
- ⁴⁶ T. Senthil, L. Balents, S. Sachdev, A. Vishwanath, and M. P. A. Fisher, “Quantum criticality beyond the Landau-Ginzburg-Wilson paradigm,” *Phys. Rev. B* **70**, 144407 (2004) [arXiv:cond-mat/0312617].
- ⁴⁷ A. M. Polyakov, “Compact gauge fields and the infrared catastrophe,” *Phys. Lett. B* **59**, 82 (1975).
- ⁴⁸ L. Fu, S. Sachdev, and C. Xu, “Geometric phases and competing orders in two dimensions,” *Phys. Rev. B* **83**, 165123 (2011) [arXiv:1010.3745 [cond-mat.str-el]].
- ⁴⁹ A. G. Abanov and P. B. Wiegmann, “Theta terms in nonlinear sigma models,” *Nucl. Phys.* **B570**, 685-698 (2000) [arXiv:hep-th/9911025].
- ⁵⁰ A. Tanaka and Xiao Hu, “Many-body spin Berry phases emerging from the π -flux state:

- antiferromagnetic/valence-bond-solid competition,” *Phys. Rev. Lett.* **95**, 036402 (2005) [arXiv:cond-mat/0501365].
- ⁵¹ T. Senthil and M. P. A. Fisher, “Competing orders, non-linear sigma models, and topological terms in quantum magnets,” *Phys. Rev. B* **74**, 064405 (2006) [arXiv:cond-mat/0510459].
- ⁵² H. Yao and D. -H. Lee, “Topological insulators and topological non-linear sigma models,” *Phys. Rev. B* **82**, 245117 (2010) [arXiv:1003.2230 [cond-mat.str-el]].
- ⁵³ M. A. Metlitski, and S. Sachdev, “Quantum phase transitions of metals in two spatial dimensions: II. Spin density wave order,” *Phys. Rev.* **B82**, 075128 (2010) [arXiv:1005.1288 [cond-mat.str-el]].
- ⁵⁴ M. A. Metlitski, and S. Sachdev, “Instabilities near the onset of spin density wave order in metals,” *New Journal of Physics* **12**, 105007 (2010) [arXiv:1007.1968 [cond-mat.str-el]].
- ⁵⁵ O. I. Motrunich, “Variational study of triangular lattice spin-1/2 model with ring exchanges and spin liquid state in κ -(ET)₂Cu₂(CN)₃,” *Phys. Rev. B* **72**, 045105 (2005) [arXiv:cond-mat/0412556].
- ⁵⁶ S.-S. Lee and P. A. Lee, “U(1) Gauge Theory of the Hubbard Model : Spin Liquid States and Possible Application to κ -(BEDT-TTF)₂Cu₂(CN)₃,” *Phys. Rev. Lett.* **95**, 036403 (2005) [arXiv:cond-mat/0502139].
- ⁵⁷ T. Senthil, “Theory of a continuous Mott transition in two dimensions,” *Phys. Rev. B* **78**, 045109 (2008) [arXiv:0804.1555 [cond-mat.str-el]].
- ⁵⁸ S. Florens and A. Georges, “Slave-rotor mean field theories of strongly correlated systems and the Mott transition in finite dimensions,” *Phys. Rev. B* **70**, 035114 (2004) [arXiv:cond-mat/0404334].
- ⁵⁹ M. Hermele, T. Senthil, M. P. A. Fisher, P. A. Lee, N. Nagaosa, and X.-G. Wen, “On the stability of U(1) spin liquids in two dimensions,” *Phys. Rev. B* **70**, 214437 (2004) [arXiv:cond-mat/0404751].
- ⁶⁰ Sung-Sik Lee, “Stability of the U(1) spin liquid with spinon Fermi surface in 2+1 dimensions,” *Phys. Rev. B* **78**, 085129 (2008) [arXiv:0804.3800 [cond-mat.str-el]].
- ⁶¹ Sung-Sik Lee, “Low energy effective theory of Fermi surface coupled with U(1) gauge field in 2+1 dimensions,” *Phys. Rev. B* **80**, 165102 (2009) [arXiv:0905.4532 [cond-mat.str-el]].
- ⁶² M. A. Metlitski, and S. Sachdev, “Quantum phase transitions of metals in two spatial dimensions: I. Ising-nematic order,” *Phys. Rev.* **B82**, 075127 (2010) [arXiv:1001.1153 [cond-mat.str-el]].
- ⁶³ D. F. Mross, J. McGreevy, H. Liu, and T. Senthil, “A controlled expansion for certain non-Fermi liquid metals,” *Phys. Rev. B* **82**, 045121 (2010) [arXiv:1003.0894 [cond-mat.str-el]].
- ⁶⁴ R. K. Kaul, M. A. Metlitski, S. Sachdev and C. Xu, “Destruction of Neel order in the cuprates by electron-doping,” *Phys. Rev. B* **78**, 045110 (2008) [arXiv:0804.1794 [cond-mat.str-el]].
- ⁶⁵ R. K. Kaul, Y. B. Kim, S. Sachdev, and T. Senthil, “Algebraic Charge Liquids,” *Nature Physics* **4**, 28 (2008) [arXiv:0706.2187 [cond-mat.str-el]].

- ⁶⁶ R. K. Kaul, A. Kolezhuk, M. Levin, S. Sachdev, and T. Senthil, “Hole dynamics in an antiferromagnet across a deconfined quantum critical point,” *Phys. Rev. B* **75**, 235122 (2007) [arXiv:cond-mat/0702119].
- ⁶⁷ Y. Qi and S. Sachdev, “Effective theory of Fermi pockets in fluctuating antiferromagnets,” *Phys. Rev. B* **81**, 115129 (2010) [arXiv:0912.0943 [cond-mat.str-el]].
- ⁶⁸ E. G. Moon and S. Sachdev, “The underdoped cuprates as fractionalized Fermi liquids: transition to superconductivity,” arXiv:1010.4567 [cond-mat.str-el].
- ⁶⁹ T. C. Ribeiro and X.-G. Wen, “Doped carrier formulation and mean-field theory of the t - t' - t'' - J model,” *Phys. Rev. B* **74**, 155113 (2006) [arXiv:0705.2261 [cond-mat.str-el]].
- ⁷⁰ Ying Ran and X.-G. Wen, “Dichotomy in underdoped high T_c superconductors and spinon-dopon approach to t - t' - t'' - J model,” arXiv:cond-mat/0611034.
- ⁷¹ T. C. Ribeiro and X.-G. Wen, “Electromagnetic response of high- T_c superconductors – the slave-boson and doped-carrier theories,” *Phys. Rev. B* **77**, 144526 (2007) [arXiv:0705.2261 [cond-mat.str-el]].
- ⁷² S. Powell, S. Sachdev, and H. P. Büchler, “Depletion of the Bose-Einstein condensate in Bose-Fermi mixtures,” *Phys. Rev. B* **72**, 024534 (2005) [arXiv:cond-mat/0502299].
- ⁷³ P. Coleman, I. Paul, and J. Rech, “Sum rules and Ward identities in the Kondo lattice,” *Phys. Rev. B* **72**, 094430 (2005) [arXiv:cond-mat/0503001].
- ⁷⁴ T. Faulkner, H. Liu, J. McGreevy, and D. Vegh, “Emergent quantum criticality, Fermi surfaces, and AdS(2),” arXiv:0907.2694 [hep-th].
- ⁷⁵ T. Faulkner and J. Polchinski, “Semi-Holographic Fermi Liquids,” arXiv:1001.5049 [hep-th].
- ⁷⁶ S. A. Hartnoll, J. Polchinski, E. Silverstein, and D. Tong, “Towards strange metallic holography,” *JHEP* **1004**, 120 (2010) [arXiv:0912.1061 [hep-th]].
- ⁷⁷ S. S. Gubser and F. D. Rocha, *Phys. Rev. D* **81**, 046001 (2010).
- ⁷⁸ C. Charmousis, B. Gouteraux, B. S. Kim, E. Kiritsis, and R. Meyer, “Effective Holographic Theories for low-temperature condensed matter systems,” *JHEP* **1011**, 151 (2010) [arXiv:1005.4690 [hep-th]].
- ⁷⁹ S. A. Hartnoll and A. Tavanfar, “Electron stars for holographic metallic criticality,” *Phys. Rev. D* **83**, 046003 (2011) [arXiv:1008.2828 [hep-th]].
- ⁸⁰ S. A. Hartnoll, D. M. Hofman, and A. Tavanfar, “Holographically smeared Fermi surface: Quantum oscillations and Luttinger count in electron stars,” arXiv:1011.2502 [hep-th].
- ⁸¹ X. Arsiwalla, J. de Boer, K. Papadodimas, and E. Verlinde, “Degenerate Stars and Gravitational Collapse in AdS/CFT,” *JHEP* **1101**, 144 (2011) [arXiv:1010.5784 [hep-th]].
- ⁸² K. Goldstein, S. Kachru, S. Prakash, and S. P. Trivedi, “Holography of Charged Dilaton Black Holes,” *JHEP* **1008**, 078 (2010) [arXiv:0911.3586 [hep-th]].
- ⁸³ K. Goldstein, N. Iizuka, S. Kachru, S. Prakash, S. P. Trivedi, and A. Westphal, “Holography of Dyonically Charged Dilaton Black Branes,” *JHEP* **1010**, 027 (2010) [arXiv:1007.2490 [hep-th]].
- ⁸⁴ S. Kachru, A. Karch, and S. Yaida, “Adventures in Holographic Dimer Models,” *New J. Phys.*

- 13**, 035004 (2011) [arXiv:1009.3268 [hep-th]].
- ⁸⁵ D. Nickel and D. T. Son, “Deconstructing holographic liquids,” arXiv:1009.3094 [hep-th].
- ⁸⁶ A. Karch, D. T. Son, and A. O. Starinets, “Holographic Quantum Liquid,” Phys. Rev. Lett. **102**, 051602 (2009) [arXiv:0806.3796 [hep-th]].
- ⁸⁷ I. Heemskerk and J. Polchinski, “Holographic and Wilsonian Renormalization Groups,” arXiv:1010.1264 [hep-th].
- ⁸⁸ T. Faulkner, H. Liu, and M. Rangamani, “Integrating out geometry: Holographic Wilsonian RG and the membrane paradigm,” arXiv:1010.4036 [hep-th].
- ⁸⁹ L. B. Ioffe and A. I. Larkin, “Gapless fermions and gauge fields in dielectrics,” Phys. Rev. B **39**, 8988 (1989).